

Surface and Build-up Region Dose Measurement in Head and Neck Region using Radio
- Photoluminescent Glass Dosimeter



A Thesis Submitted in Partial Fulfillment of the Requirements
for the Degree of Master of Science in Medical Physics

Department of Radiology

FACULTY OF MEDICINE

Chulalongkorn University

Academic Year 2020

Copyright of Chulalongkorn University

การวัดปริมาณรังสีที่ผิวและบริเวณที่มีการเพิ่มของปริมาณรังสีบริเวณศีรษะและลำคอโดยใช้เครื่องวัด
รังสีชนิดแก้ว



วิทยานิพนธ์นี้เป็นส่วนหนึ่งของการศึกษาตามหลักสูตรปริญญาวิทยาศาสตรมหาบัณฑิต
สาขาวิชาฟิสิกส์การแพทย์ ภาควิชารังสีวิทยา
คณะแพทยศาสตร์ จุฬาลงกรณ์มหาวิทยาลัย
ปีการศึกษา 2563
ลิขสิทธิ์ของจุฬาลงกรณ์มหาวิทยาลัย

โซนมัม โซกิ : การวัดปริมาณรังสีที่ผิวและบริเวณที่มีการเพิ่มของปริมาณรังสีบริเวณศีรษะและลำคอ โดยใช้เครื่องวัดรังสีชนิดแก้ว. (Surface and Build-up Region Dose Measurement in Head and Neck Region using Radio - Photoluminescent Glass Dosimeter) อ.ที่ปรึกษาหลัก : ผศ. ทวีป แสงแห่งธรรม

ปัจจุบันมีการใช้เครื่องวัดรังสีแก้ว radio-photoluminescent glass (RPLGD) ทางการค้าเพิ่มขึ้นเนื่องจากมีลักษณะเฉพาะหลายอย่างในการใช้วัดปริมาณรังสีที่ดีกว่าเครื่องวัดรังสีชนิดอื่น วัตถุประสงค์ของงานวิจัยนี้คือ เพื่อประเมินความเป็นไปได้ในการนำเครื่องวัดรังสีแก้ว GD-302M วัดปริมาณรังสีที่ผิวและช่วงที่ปริมาณรังสีเพิ่มขึ้น (buildup) บริเวณศีรษะและลำคอ เริ่มจากการศึกษาคุณสมบัติต่าง ๆ ในการวัดปริมาณรังสีของเครื่องวัดแก้วจากนั้นทำการเปรียบเทียบปริมาณรังสีที่ผิวและช่วงที่ปริมาณรังสีที่เพิ่มขึ้นระหว่างเครื่องวัดแก้วและฟิล์ม EBT3 ในแพนทอมน้ำที่ความลึก 0, 2, 3, 5, 10 และ 15 มม จากโพตอนพลังงาน 6 เมกะโวลต์ และทำการตรวจสอบแผนการรักษาผู้ป่วยมะเร็งหลังโพรงจมูกเทคนิค 3D-CRT และ VMAT ด้วยเครื่องวัดรังสีแก้วในแพนทอม Rando ที่ความลึก 5 และ 10 มม ผลการศึกษาพบว่าความสม่ำเสมอในการวัดปริมาณรังสีของเครื่องวัดรังสีแก้วอยู่ภายใน 1.1% สัญญาณที่อ่านได้แปรผันตรงกับค่าปริมาณรังสีมีค่า R^2 ที่ 0.999 ในส่วนของอัตราปริมาณรังสี การอ่านค่าซ้ำการตอบสนองของสัญญาณที่มุมต่างๆและพลังงานอยู่ภายใน 3% นอกจากนี้มีการจางหายของสัญญาณน้อยกว่า 3% ในเวลา 4 สัปดาห์เมื่อทำการเปรียบเทียบปริมาณรังสีระหว่างเครื่องวัดรังสีแก้วกับฟิล์ม EBT3 ในแพนทอมน้ำพบว่าค่าที่ได้มีความสอดคล้องกันดีในบริเวณช่วงที่มีปริมาณรังสีเพิ่มขึ้นแต่เครื่องวัดรังสีแก้วให้ค่าปริมาณรังสีสูงกว่าปกติที่ผิวแพนทอมเนื่องจากความหนาของปลอกหุ้มเมื่อทำการตรวจสอบปริมาณรังสีจากแผนการรักษาในแพนทอม Rando พบว่าเครื่องวัดรังสีแก้วให้ค่าปริมาณรังสีเฉลี่ยสูงกว่าค่าจากเครื่องวางแผนการรักษาทั้งในเทคนิค 3DCRT และ VMAT โดยค่าความแตกต่างเฉลี่ยของปริมาณรังสีจากการวัดด้วยเครื่องวัดรังสีแก้วกับค่าจากเครื่องวางแผนการรักษาอยู่ที่ $-0.18 \pm 1.21\%$ ที่ความลึก 5 มม, $2.40 \pm 1.49\%$ ที่ความลึก 10 มม สำหรับเทคนิค 3D-CRT, และมีความแตกต่างเฉลี่ยที่ $4.74 \pm 1.12\%$ ที่ความลึก 5 มม และ $3.44 \pm 4.41\%$ ที่ความลึก 10 มม สำหรับเทคนิค VMAT ตามลำดับโดยสรุป เครื่องวัดรังสีแก้วไม่เหมาะสำหรับการนำมาใช้วัดปริมาณรังสีที่ผิวแต่สามารถนำมาใช้วัดปริมาณรังสีบริเวณที่มีปริมาณรังสีเพิ่มขึ้นได้อย่างดี

สาขาวิชา ฟิสิกส์การแพทย์
ปีการศึกษา 2563

ลายมือชื่อนิสิต
ลายมือชื่อ อ.ที่ปรึกษาหลัก

6270001930 : MAJOR MEDICAL PHYSICS

KEYWORD: SURFACE DOSE, BUILD-UP REGION, RPLGD, EBT3, TPS

Sonam Choki : Surface and Build-up Region Dose Measurement in Head and Neck Region using Radio - Photoluminescent Glass Dosimeter. Advisor: Asst. Prof. TAWEAP SANGHANGTHUM, Ph.D.

The use of commercially available radio-photoluminescent glass dosimeter (RPLGD) for radiation measurement has increased in recent years. It has been shown to have superior dosimetric characteristics as compared to other dosimeters. The purpose of this research is to evaluate the suitability of the GD-302M glass dosimeter for surface and build-up region dose measurement in head and neck region. The glass dosimeter was analyzed for its dosimetric properties in photon beam. Then, the study was performed for surface and build-up region dose comparison between EBT3 film and RPLGD in solid water phantom at 0, 2, 3, 5, 10 and 15mm depths of 6 MV beams. In addition, 3D-CRT and VMAT plans for nasopharyngeal carcinoma were transferred to a Rando phantom for verification of build-up region dose at 5 and 10mm depths. The results found that uniformity obtained in this study was within 1.1%. The dose-response was linear with R^2 of 0.999. Dose rate, reproducibility, angular and energy dependence were found to be within 3.0%. Moreover, fading effect was less than 3% over 4 weeks. The dose in homogeneous solid water phantom showed good agreement between RPLGD and EBT3 film in build-up region. However, RPLGD showed over response of signal at the surface due to the thickness of its holder. The verification in Rando phantom illustrated that build-up region doses were higher in TPS calculation compared to RPLGD measurements both in 3DCRT and VMAT. The average dose differences between measurements and calculations were $-0.18 \pm 1.21\%$ and $2.40 \pm 1.49\%$ at 5 mm and 10 mm depth for 3D-CRT, and $4.74 \pm 1.12\%$ and $3.44 \pm 4.41\%$ at 5 mm and 10 mm depth for VMAT, respectively. In conclusion, RPLGD is less suitable for surface dose measurement but has good potential to be used as an in-vivo dosimeter in build-up dose measurements.

Field of Study: Medical Physics

Student's Signature

Academic Year: 2020

Advisor's Signature

ACKNOWLEDGEMENTS

First and foremost, I would like to express immense gratitude to my advisor Assistant Professor Dr. Taweap Sanghangthum, Division of Radiation Oncology, Department of Radiology, Faculty of Medicine, Chulalongkorn University, for his continued support, guidance and invaluable advice throughout the process in successfully completing this research. I am equally grateful to Mrs. Chulee Vannavijit, my co-advisor who helped me with my experiments and in shaping my experimental methods with constructive comments.

I would also like to extend my sincere gratitude to Associate Professor Sivalee Suriyapee, Division of Radiation Oncology, Department of Radiology, Faculty of Medicine, Chulalongkorn University, who helped me in modeling my thoughts from different perspectives with her profound knowledge and experiences.

I am also grateful to all the medical physicists from the Department of Radiation Oncology, King Chulalongkorn Memorial Hospital for your time, energy, and expertise through this entire process.

I would like to thank Associate Professor Dr. Anchali Krisanachinda, Division of Nuclear Medicine, Department of Radiology, Faculty of Medicine, Chulalongkorn University, for being a huge supporter since the day I enrolled and giving me this wonderful opportunity to be a part of the Medical Physics Program at Chulalongkorn University.

My sincere thanks go to Professor Dr. Kosuke Matsubara, Kanazawa University, for examining this thesis and also offering valuable suggestions as an insightful mentor for all.

I am thankful to all my professors, staffs and my friends from MPCU 17 batch of medical physics fraternity at Chulalongkorn University for rendering their support and kindness. I would like to thank my country, Bhutan and the government of Thailand for their generous scholarship. Last but not the least, I would like to thank my family and my husband who have stuck with me through thick and thin.

Sonam Choki

TABLE OF CONTENTS

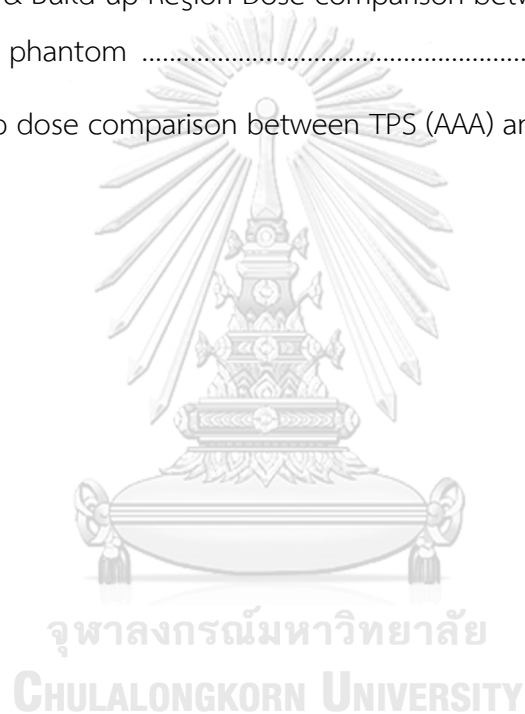
	Page
.....	iii
ABSTRACT (THAI)	iii
.....	iv
ABSTRACT (ENGLISH)	iv
ACKNOWLEDGEMENTS	v
TABLE OF CONTENTS	vi
LIST OF TABLES	ix
LIST OF FIGURES.....	x
LIST OF ABBREVIATIONS	xii
CHAPTER 1 INTRODUCTION.....	1
1.1 Background and Rationale	1
1.2 Research Objective	2
CHAPTER 2 REVIEW OF RELATED LITERATURE.....	3
2.1 Theory.....	3
2.1.1 Head and Neck Cancer.....	3
2.1.2 Treatment and Clinical Trials.....	4
2.1.3 Treatment Techniques for H&N Radiotherapy	4
2.1.3.1 Three-Dimensional Conformal Radiotherapy.....	5
2.1.3.2 Volumetric Modulated Arc Therapy (VMAT).....	5
2.1.4 Surface Dose	7
2.1.5 Dose Calculation Algorithm.....	8

2.1.5.1 Analytical Anisotropic Algorithm (AAA).....	9
2.1.6 Dosimetry Theory	9
2.1.6.1 Radiochromic Film	9
2.1.6.2 Radio-photoluminescent Glass Dosimeter (RPLGD).....	11
2.2 Related Literatures.....	13
CHAPTER 3 RESEARCH METHODOLOGY.....	16
3.1 Research Design.....	16
3.2 Research Question	16
3.3 Research Design Model.....	17
3.4 Conceptual Framework.....	18
3.5 Materials	19
3.6 Methods.....	26
3.7 Patient Analysis.....	32
3.8 Outcome Measurements.....	33
3.9 Sample Size	33
3.10 Statistical Analysis.....	34
3.11 Expected Benefit.....	34
3.12 Ethical Consideration	34
CHAPTER 4 RESULTS.....	36
4.1 Dosimetric Characteristics of RPLGD.....	36
4.1.1 Uniformity.....	36
4.1.2 Reproducibility of the dosimeter reader	36
4.1.3 Linearity.....	37
4.1.4 Repetition Rate Response	38

4.1.5 Energy Response.....	38
4.1.6 Angular Dependence	39
4.1.7 Fading Effect	40
4.2 EBT3 Calibration	40
4.3 Surface & Build-up Region Doses in Homogeneous Solid Water Phantom.....	41
4.4 Verification of Plans in H&N Rando Phantom using RPLGD.....	42
CHAPTER 5 DISCUSSION AND CONCLUSION.....	45
5.1 Discussion.....	45
5.1.1 Dosimetric Characteristics of RPLGD.....	45
5.1.2 Surface and Build-up region Dose Measurement.....	46
5.1.3 Verification of Plans in Rando Phantom with RPLGD.....	47
5.2 Conclusion	48
APPENDIX	49
REFERENCES.....	51
VITA	55

LIST OF TABLES

	Page
Table 2. 1 Correction factors necessary to scale the dose measured at the effective point.....	14
Table 3. 1 The experimental conditions in homogeneous solid water phantom.....	28
Table 4. 1 Energy response of RPLGD	39
Table 4. 2 Surface & Build-up Region Dose comparison between EBT3 and RPLGD in solid water phantom	42
Table 4. 3 Build-up dose comparison between TPS (AAA) and RPLGD	44



LIST OF FIGURES

	Page
Figure 2. 1 Major anatomical sites of head and neck.....	3
Figure 2. 2 H&N treatment plan for 3D-CRT technique.....	5
Figure 2.3 H&N treatment plan for VMAT technique	6
Figure 2.4 Structure of GAFChromic EBT3 Dosimetry Film	10
Figure 2.5 Three types of RPLGD	12
Figure 2.6 The energy levels of RPLGD.....	12
Figure 3.1 Research Design Model.....	17
Figure 3.2 Conceptual Framework.....	18
Figure 3.3 Varian RapidArc	19
Figure 3.4 Varian Clinac 23EX	20
Figure 3.5 SIEMENS CT Scanner	20
Figure 3.6 Solid water phantom	21
Figure 3.7 Disk phantom	21
Figure 3.8 Alderson Rando Phantom	22
Figure 3.9 Tissue Mimicking Bolus	22
Figure 3.10 RPLGD 302-M and holder	23
Figure 3.11 Gafchromic EBT3 Film	24
Figure 3.12 Epson perfection flat-bed CCD scanner	25
Figure 3.13 Varian Eclipse TPS	25
Figure 3.14 RPLGD set-up for dosimetric characteristics study.....	26
Figure 3.15 EBT3 film calibration set-up.....	29
Figure 3.16 EBT3 set-up for dose measurement.....	29
Figure 3.17 RPLGD set-up for dose measurement.....	30
Figure 3.18 CT scanning of rando phantom	31

Figure 3.19 Rando phantom set-up in the treatment machine	31
Figure 3.20 The calculated doses recorded for VMAT; (a) 5 mm, (b) 10 mm	32
Figure 3.21 Ethical consideration certificate	35
Figure 4.1 The uniformity of 25 RPLGDs for 6-MV photon beams	36
Figure 4.2 The relative response of FDG-1000 reader system from 10 RPLGDs	37
Figure 4.3 The linearity response of RPLGD	37
Figure 4.4 The Rep. rate response of RPLGD	38
Figure 4.5 The angular dependence of RPLGD at various gantry angles	39
Figure 4.6 The fading response of RPLGD	40
Figure 4.7 Film calibration curve	40
Figure 4.8 Surface & Build-up Region Dose comparison between EBT3 and RPLGD in solid water phantom	42
Figure 4.9 Build-up dose measurement and calculation for 3DCRT	43
Figure 4.10 Build-up dose measurement and calculation for VMAT	44

LIST OF ABBREVIATIONS

Abbreviation Terms

2D	Two-dimensional
3DCRT	Three-dimensional conformal radiotherapy
AAA	Analytical Anisotropic Algorithm
AXB	Acuros XB
CCD	Charge- coupled device
CTV	Clinical target volume
DICOM	Digital Imaging and Communications in Medicine
EBT	External beam therapy
FIF	Field in field
GD	Glass dosimeter
H&N	Head and Neck
IAEA	International Atomic Energy Agency
IMB	Intensity-modulated beams
IMRT	Intensity-modulated radiation therapy
MC	Monte carlo
MLC	Multi-leaf collimator
MOSFET	Metal oxide semiconductor field effect transistors
MU	Monitor unit
MV	Megavoltage
NTCP	Normal tissue complication probability

OAR	Organs-at-risk
PDD	Percentage depth dose
PMMA	Poly methyl methacrylate
PTV	Planning target volume
RPLGD	Radio-photoluminescent glass dosimeter
SSD	Source to skin distance
TBI	Total body irradiation
TCP	Tumor control probability
TLD	Thermoluminescent dosimeter
TRS	Technical report series
TPS	Treatment planning system
VMAT	Volumetric modulated arc therapy

CHAPTER 1

INTRODUCTION

1.1 Background and Rationale

In radiotherapy, megavoltage photons generated by medical linear accelerators are used for the treatment of cancer and these megavoltage X-rays have a skin-sparing effect, whereby the maximum dose is deposited in the deep tissues than in the skin.(1)Therefore, the dose at the surface should be negligible but it is not achieved. This is because therapeutic photon beam has electron contamination in the first few millimeters of skin caused by photon interactions in air or interactions with collimator and treatment head in the path of the beam. (2, 3) The surface dose is also affected by various treatment parameters such as field size, source to skin distance (SSD), beam angle, beam energy, and beam modifiers such as wedges, blocks and multi-leaf collimator (MLC) systems. (4) Charged particle equilibrium does not exist at this depth and the dose gradient is high in the buildup region. Therefore, accurate knowledge of surface dose is important, but the measurement at such depths is a challenging issue. Skin dosimetry is further complicated by the different structures of the skin (including basal and dermal layers), the depth of which varies not only between patients, but also between locations on a given patient. Knowledge of surface dose is important especially when skin becomes a limiting factor in dose delivery to the deep-seated tumors and when they become part of the target volume in the treatment area.(5) This can result in excessive radiation dose to the skin, thereby causing early radiation effects such as erythema or late effects such as hypoxia, fibrosis, etc.

The results of surface dose measurements may vary with the type of dosimeters used due to its own specific physical property. Dosimeters are generally divided into two categories, active and passive dosimeters. Active dosimeters require power and can provide real time readout. This category includes gas-filled counters, scintillation counters, and semi-conductor, etc. As for passive dosimeters, radiation interaction is detected through certain physical processes after radiation interacts with medium in the

dosimeter. They are often used as periodic radiation monitor for people working in the radiation environment to monitor the cumulated dose and the types of radiation. They can be used as personal dose measurement, long-term environmental radiation dose monitor, etc. The film badge, Thermoluminescence Dosimeter (TLD), Optically Stimulated Luminescence Dosimeter (OSLD), Film Dosimeters, and Radiophotoluminescent Glass Dosimeter (RPLGD) are commonly used as passive dosimeters. (6)

Surface and build-up regions can be measured most accurately with extrapolation chamber, but not every institution has this equipment and the process takes a very long time. The use of commercially available RPLGD for radiation measurement has increased in recent years. Previous study showed that the glass dosimeter can be used as an accurate and reproducible dosimeter for skin dose measurements. (7) Radiochromic film is suitable dosimeter for surface dosimetry owing to its high spatial resolution and low spectral sensitivity. These characteristics make the films suitable for the measurement in regions of steep dose gradient. (8, 9) However, films are difficult to form to curved surfaces such as breast and head and neck region. With increased skin reactions from radiotherapy in patients with head and neck cancer, questions have arisen as to the selection of a suitable dosimeter for surface and build-up dose measurement. Therefore, in this research, we are going to compare glass dosimeter to Gafchromic EBT3 film as the reference dosimeter in the measurement of surface and build-up region dose.

1.2 Research Objective

To evaluate the suitability of the Glass Dosimeter (GD-302M) for surface and build-up doses measurement in head and neck region.

CHAPTER 2 REVIEW OF RELATED LITERATURE

2.1 Theory

2.1.1 Head and Neck Cancer

“Head and neck cancer” is the term used to describe a number of different malignant tumors that develop in or around the throat, larynx, nose, sinuses, and mouth. Squamous cell carcinoma of the head and neck region constitutes approximately 90% of all head and neck cancers. This type of cancer begins in the flat squamous cells that make up the thin layer of tissue on the surface of the structures in the head and neck. Directly beneath this lining, which is called the epithelium, some areas of the head and neck have a layer of moist tissue, called the mucosa. If a cancer is only found in the squamous layer of cells, it is called carcinoma in situ. If the cancer has grown beyond this cell layer and moved into the deeper tissue, then it is called invasive squamous cell carcinoma (10) The most common subsites in Thailand are oral cavity followed by nasopharynx and other parts of head and neck. (Fig 2.1) (11)

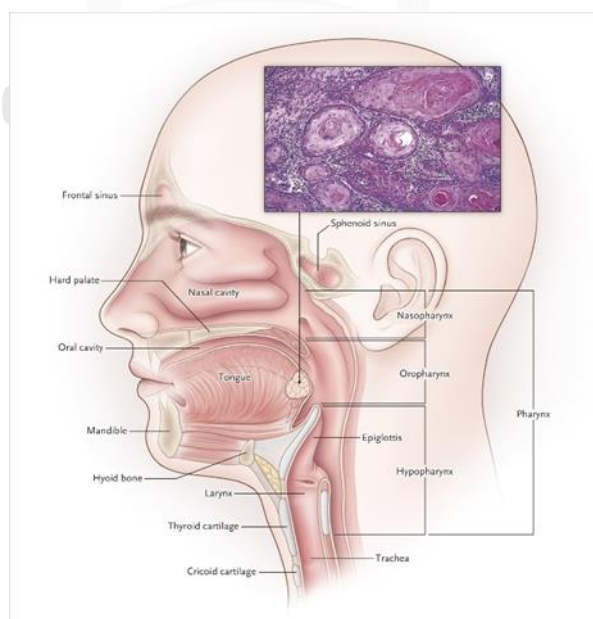


Figure 2.1 Major anatomical sites of head and neck.

2.1.2 Treatment and Clinical Trials

Head and neck cancer is often complex, with many different sites and staging systems. However, current therapy offers several alternatives, including surgery, radiation and chemotherapy, either alone or in combination. Combined treatment modality is becoming the principal method of treating patients with locally advanced head and neck cancer cases.(12) Radiation may cause side effects such as acute toxicity, mucositis and dry mouth, difficulty in swallowing, mouth sores, and skin reactions (e.g., redness, itching, burning). Some patients may also want to explore the possibility of participating in clinical trials. Clinical trials may offer cutting-edge technology in treatment and also provide oncologists, surgeons, and radiation oncologists the opportunity to further refine and improve treatment options. For better outcomes and increased survival, multidisciplinary care which includes support from dental, nutritional, and speech and language services, as well as audiometry, occupational and physical therapy, and psychosocial services are also required.(11)

2.1.3 Treatment Techniques for H&N Radiotherapy

There are different modalities in radiotherapy used in the treatment of head and neck cancer. There are two kinds of radiotherapy treatment, external beam and internal (brachytherapy) beam therapy. Brachytherapy can be used in few cases of head and neck region but it is rarely employed alone. There are many techniques in external beam therapy, which has evolved over time such as conventional radiotherapy (2D), three-dimensional conformal radiotherapy (3D-CRT), intensity-modulated radiotherapy (IMRT), and volumetric modulated arc therapy (VMAT). The treatment technique chosen depends primarily on the size, location and grade of the primary tumor; the extend of nodal involvement and the prognosis of the treatment. Out of many techniques, two of these used in our dose comparison are 3D-CRT and VMAT.

2.1.3.1 Three-Dimensional Conformal Radiotherapy

Three-dimensional conformal radiotherapy means treatments that are based on 3D anatomic information and use treatment fields that conform as closely as possible to the target volume in order to deliver adequate dose to the tumor and minimum possible dose to normal tissue. The concept of conformal dose distribution also means to fulfill clinical objectives such as maximizing tumor control probability (TCP) and minimizing normal tissue complication probability (NTCP). Thus, the 3D-CRT technique encompasses both the physical and biologic rationales in achieving the desired clinical results. (13) Although, highly modulated techniques such as IMRT and VMAT yield much better results than 3DCRT in sparing organs-at-risk (OARs), these techniques cannot be universally used, due to unavailability of adequate equipment, organization, or patient status. Therefore, 3D-CRT is still widely used to treat H&N cancers, in spite of its evident limitations when compared with highly modulated techniques. (14) Field-in-Field (FIF) is one of the commonly applied techniques in 3D-CRT for H&N cancer. (Fig 2.2)

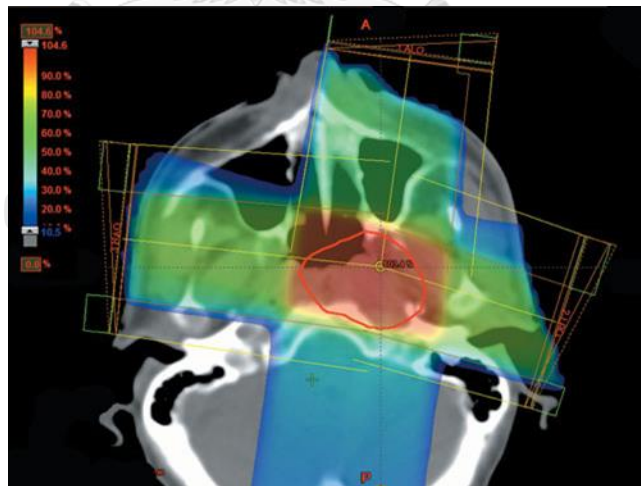


Figure 2.2 H&N treatment plan for 3D-CRT technique.

2.1.3.2 Volumetric Modulated Arc Therapy (VMAT)

In the traditional external beam photon radiation therapy, most treatments are delivered with radiation beams that are of uniform intensity across the field. The term IMRT refers to a radiation therapy technique in which a nonuniform fluence is delivered to the patient from any given position of the treatment beam to optimize the composite dose distribution. The treatment criteria for plan optimization are specified by the planner and the optimal fluence profiles for a given set of beam directions are determined through “inverse planning”. The fluence files thus generated are electronically transmitted to the linear accelerator, which is computer controlled, that is, equipped with the required software and hardware to deliver the intensity-modulated beams (IMBs) as calculated.(13) Volumetric modulated arc therapy is more advanced compared with conventional static IMRT in which it allows for simultaneous variation of three parameters during treatment delivery, *i.e.*, gantry rotation speed, treatment aperture shape via movement of MLC leaves and dose rate. (Fig 2.3) (15)

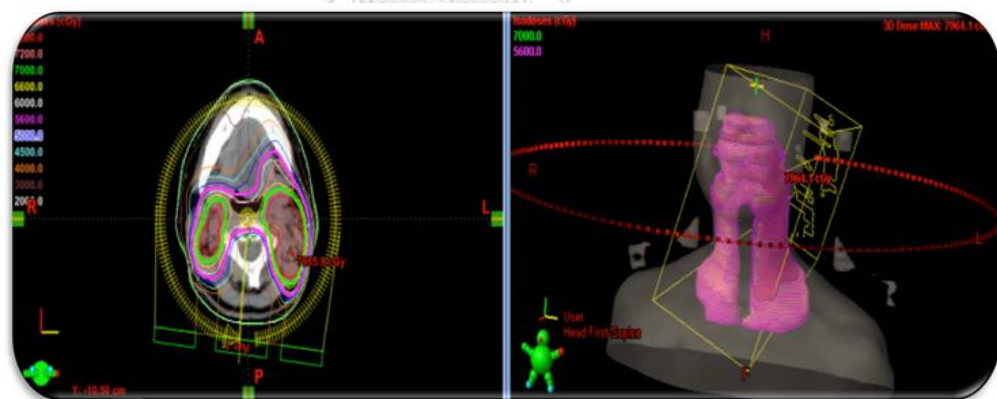


Figure 2.3 H&N treatment plan for VMAT technique.

2.1.4 Surface Dose

Dose deposited at the boundary between the air and the phantom is defined as the surface dose.(16) For megavoltage photon beams the surface dose is generally much lower than the maximum dose, which occurs at a depth of maximum dose (z_{max}) beneath the patient's surface. In megavoltage photon beams the surface dose depends on the beam energy and field size. Larger the photon beam energy, the lower the surface dose and for a given beam energy the surface dose increases with the field size. An important advantage of megavoltage beams over orthovoltage and superficial beams is its skin sparing effect where low surface dose is deposited as compared to the maximum dose. The surface dose represents contributions to the dose from photons scattered from the collimators, flattening filter and air, photons backscattered from the patient, high energy electrons produced by photon interactions in air and any shielding structures in the vicinity of the patient.(17)

Accurate knowledge of dose to superficial tissues is necessary to ensure that shallow targets receive the prescribed dose while the dose to normal tissue is within tolerance. (18, 19) However, measurement of surface dose is a challenging issue mainly because of the inaccuracy of most TPSs in the buildup region.(20) Although, several dosimeters are currently used in radiotherapy for surface skin dose estimation, finding a suitable dosimeter to measure surface dose is still difficult due to lack of electronic equilibrium in that region.

Some of the commonly used dosimeters for surface dose estimation includes TLDs, (21) diodes, (22) and metal oxide semiconductor field effect transistors (MOSFETs) (5) which may be used to produce low resolution surface dose distributions. Radiographic or radiochromic film may be used to quantitate the distribution of surface dose in two dimensions. (23, 24) Radiochromic film has several advantages, such as tissue equivalency, high stability, self-development, and high spatial resolution. However, film is difficult to measure on surfaces that are either convex or concave regions. (25, 26) In these situations, a more flexible or suitable dosimeter is desirable. The use of RPLGD have increased recently and it has been shown to have good potential in radiation measurement.

2.1.5 Dose Calculation Algorithm

Dose calculation algorithms are the most critical software component in a computerized treatment planning system (TPS). They are responsible for the correct representation of dose in the patient, and may be linked to beam time or monitor unit (MU) calculations. Dose calculations have evolved from simple 2-D calculations, to partial 3-D point kernel methods, to full 3-D dose models in which the histories of the primary and scattered radiation in the volume of interest are considered.[28] The accuracy of the dose delivered depends on the accuracy of treatment planning calculation algorithm.

The dose calculation algorithms in radiotherapy are classified as correction-based and model-based. The correction-based algorithms calculate the dose in a patient by correcting the measured dose distribution in a water phantom to account for beam geometry, beam modifiers, patient contours, beam aperture opening, and tissue heterogeneities. The model-based algorithms compute the dose in a patient from “first principles” using a model of radiation transport. For correction-based algorithms, the measured data are first parameterized into functions that are subsequently used to reconstitute each treatment beam used in a patient treatment plan. For model-based algorithms, the measured data are used to define the description of the beam. The fundamental difference between the two classes of algorithms is that model-based calculations do not reconstitute measured data before correcting it for the clinical situation.(27)

The advanced dose calculation in Varian Eclipse treatment planning system is undertaken by model-based dose calculation algorithms like analytical anisotropic algorithm (AAA) and Acuros XB (AXB). In this research, AAA model-based calculation algorithm was used to compare with the surface dose measured using glass dosimeter in the final part.

2.1.5.1 Analytical Anisotropic Algorithm (AAA)

The AAA dose calculation model is a 3D pencil beam convolution-superposition algorithm that has separate modeling for primary photons, scattered extra-focal photons, and electrons scattered from the beam limiting devices. Tissue heterogeneities are accounted for anisotropically in the full 3D neighborhood by the use of 13 lateral photon scatter kernels. The final dose distribution is obtained by superposition of the doses from the photon and electron convolutions. Configuration of the AAA model is based on Monte-Carlo determined basic physical parameters that are adapted to measured clinical beam data. These in turn are used to construct a phase space defining the fluence and energy spectrum of the clinical beam specific to each treatment unit. Beam modifying accessories including blocks, hard wedges, dynamic wedges, compensators, MLCs (static and dynamic) are fully supported in the dose calculation.(28)

2.1.6 Dosimetry Theory

2.1.6.1 Radiochromic Film

Overview: Radiochromic film is a substantial dosimeter for surface dosimetry, which has alleviated some problems faced with conventional radiation dosimetry. Radiochromic films have high spatial resolution and low spectral sensitivity. Also, the short measuring time and the fact that the film dosimetry is intrinsically two-dimensional and integrating in time are advantageous. These characteristics make the films suitable for the measurement in regions of steep dose gradient.[5] There are different kinds of Radiochromic film models XR-T, HS, and EBT. The EBT model GAFCHROMIC® film has been reported in many researches in surface dose measurement. The structure of EBT3 film is shown in Figure 2.4. The film is comprised of an active layer, nominally 28 μm thick, sandwiched between two 125 μm matte-polyester substrates. The active layer contains the active component, a marker dye, stabilizers and other components giving the film its near energy independent response.

The thickness of the active layer will vary slightly between different production lots.

(29)

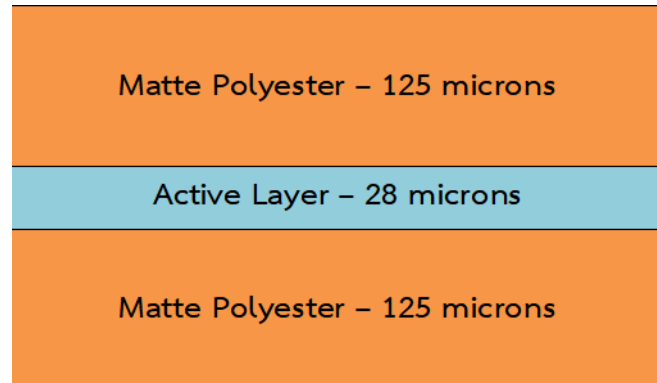


Figure 2.4 Structure of GAFChromic EBT3 Dosimetry Film.

Major features of Gafchromic EBT3 include:

- Dynamic dose range: 0.1 Gy to 20 Gy
- Optimum dose range: 0.2 Gy to 10 Gy, best suited for applications such as IMRT and VMAT
- Real time development without post-exposure treatment
- Energy-dependence: minimal response difference from 100 keV into the MV range
- New technology incorporating a marker dye in the active layer
- Enables non-uniformity correction by using multi-channel dosimetry
- Less UV/visible light sensitivity
- Stable at temperatures up to 60°C
- Near tissue equivalent
- High spatial resolution

Operation: The effective points of measurement in radiochromic films were assumed to be at the center of the sensitive layer of the film, and scaled by density, it is 0.0153 g/cm² for the EBT film. Radiochromic film changes color upon exposure to radiation. The change in optical density in GAFChromic EBT3 dosimetry film is

recommended to measure with a 48-bit (16-bit per channel) flatbed color scanner (EPSON). These are color scanners that measure the red, green and blue color components of light transmitted by the film at a color depth of 16 bit per channel. When the active component in EBT3 film is exposed to radiation, it reacts to form a blue colored polymer with absorption maxima at approximately 633 nm.

2.1.6.2 Radio-photoluminescent Glass Dosimeter (RPLGD)

Overview: RPLGD uses silver activated phosphate glass as the luminescent material. The developments of new generation RPLGD and readout system were completed in 1990 (Piesch), where the excitation source was changed from ultra-violet into pulse ultraviolet laser. There are three major types of RPLGD in the market; the SC-1 for environmental radiation dose monitor; the GD-450 for personal external radiation dose monitor; and the Dose Ace for research purposes. All those three types use FD-7 glass, manufactured by Asahi, Japan. (Fig 2.5). The Dose Ace type RPLGD is mainly for research purposes. It is a cylindrical shape with three different models; GD-302M, GD-352M, and GD-301. The GD-302M used in this study and GD-352M have a length of 12 mm and a diameter of 1.5 mm, while GD-301 has a length of 8.5 mm and a diameter of 1.5 mm. GD-301 and GD-302M, without filters in capsule, are used to measure the dose of high energy photons as in radiotherapy. However, there is a Tin filter in the capsule for GD-352M to lower the energy dependence effect. The GD-352M can be used for measuring the dose from low energy photons as in diagnostic radiology. In the process of dose readout, based on the dose values, the dose ranges are divided into two categories, low dose range (10 μ Gy – 10 Gy) and high dose range (1 Gy - 500 Gy). The readout system can automatically distinguish the dose range according to different readout magazine used by the users. (6)



Figure 2.5 Three types of RPLGD.

Operation: Figure 2.6 (6) shows the energy levels and basic principle of RPLGD. The basic principle of RPLGD is that the color centers are formed when the luminescent material inside the glass compound exposed to radiation and fluorescence are emitted from the color centers after irradiated with ultra-violet light. The excited electrons generated from the color centers return to the original color centers after emitting the fluorescence. This process is called radio-photoluminescence phenomena. Because the electrons in the color centers return to the electron traps after emitting the fluorescence, it can be re-readout for a single irradiation.

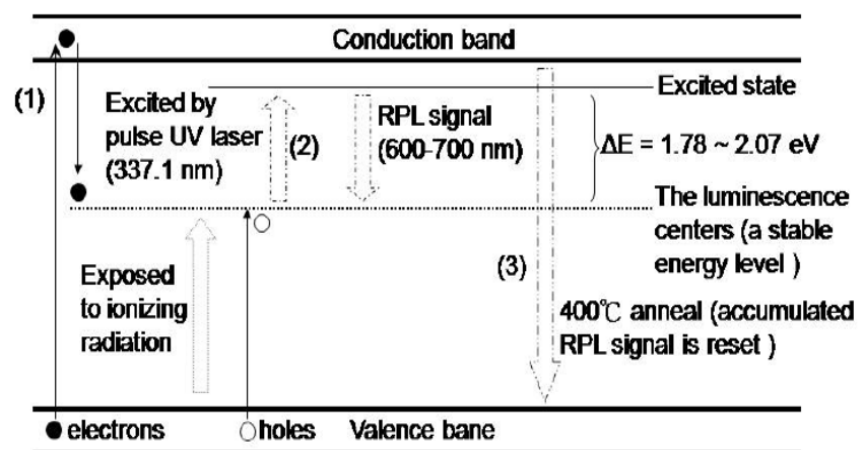


Figure 2.6 The energy levels of RPLGD.

Advantages of RPLGD system:

- RPL signal is not erased during readout. It has to be annealed at 400 °C for 30 mins to erase the signals.
- RPL dosimeter can be re-analyzed several times, and the measured data reproduced. Accumulation of the dose is also possible that may be used for registration of the lifetime dose.
- Commercially available RPL dosimeters typically cover the dose range of 10 μ Gy – 10 Gy and 1 Gy to 500 Gy.
- RPL signal exhibits very low fading and is not sensitive to the environmental temperature making it convenient in individual monitoring.
- It can handle under light and at high temperatures.
- Homogeneous composition of RPLGD ensures stable dosimetry.

2.2 Related Literatures

Devic S et al. (16) determined a correction procedure for radiochromic film in order to obtain an accurate skin dose measurement using Attix parallel-plate ionization chamber, extrapolation chamber, four types of Gafchromic films (HD-810, EBT, HS and XR-T) and TLDs. To get the correction, PDD was measured at effective point, buildup region, build-down region, field size effect was considered and also calculation with Monte Carlo simulation were performed. Their measurements suggested that within the first millimeter of the skin region, the PDD for a 6 MV photon beam and field size of 10×10 cm² increased from 14% to 40%. The skin dose correction factors for the exit skin dose due to the build-down region were negligible. For the three Gafchromic dosimetry film models, the 6 MV beam entrance skin dose measurement corrections due to their effective point of measurement were 15% for the EBT, 15% for the HS, and 16% for the XR-T model. Different dosimeters used for the surface dose estimates should be properly calibrated and necessary corrections applied in order to accurately estimate the skin dose.

The skin depth was assumed to be at the reference point of 70 μ m, and the necessary corrections for the reliable estimate of the skin dose based upon the measurements with

various Gafchromic dosimetry film models, as well as the other surface dose dosimeters, are summarized in Table 2.1.

Table 2.1 Correction factors necessary to scale the dose measured at the effective point.

	Skin 70 μm	Attix	EBT	HS	XR-T	TLD (0.15)	TLD (0.4)
PDD ($Z_{\text{eff},10,100,6}$ MV)	17.0	16.0	19.9	20.0	20.3	21.0	29.0
Correction	1.000	1.062	0.854	0.850	0.837	0.810	0.586

J.-E. Rah et al. (7) studied glass dosimeter (model GD-301) for its dosimetric characteristics, in order to evaluate its use for in vivo dosimetry. They specifically assessed overall precision of dosimetric dose data in patients who received treatment with the total body irradiation (TBI). Uniformity obtained in this study was within 1.2% (1 SD). The dose response was linear in the range of 0.5-10 Gy with R of 0.999. Dose rate, SSD, field size, angular and energy dependence were found to be within 3.0%. In vivo skin dosimetry for TBI was performed for 3 patients. Almost all of the measured values with glass dosimeter were well within $\pm 5.0\%$ of the prescription dose. Variation of doses measured by the glass dosimeter for the entrance dose in TBI was within $\pm 6.3\%$ of the mean value obtained from TLD measurements. From the above results, it is concluded that the glass dosimeter has considerable potential for use as an in vivo dosimeter.

N.N. Shehzadi et al. (30) checked the applicability of RPLGD for in vivo dosimetry in external photon beams radiotherapy. The entrance dose measurements were performed. The influence of beam set-up parameters on the entrance dose was investigated using the RPLGDs for 6 MV beam. MC simulation was performed for a correction factor related to the irradiation set-up. The entrance dose verification was performed on an Alderson Rando phantom during 64 single beam irradiations using different beam set-up. The mean ratio of the measured entrance dose using RPLGD on

the surface of the phantom to the expected dose, which was calculated by TPS was equal to 1.001 ± 0.030 . The mean ratio of the dose measured using RPLGDs inside the Alderson Rando phantom to the expected dose was equal to 1.019 ± 0.019 . This study concludes that the RPLGD is suitable for in vivo dosimetry in external photon beam radiotherapy for dose verification within $\pm 5\%$ at the clinically acceptable level.



CHAPTER 3

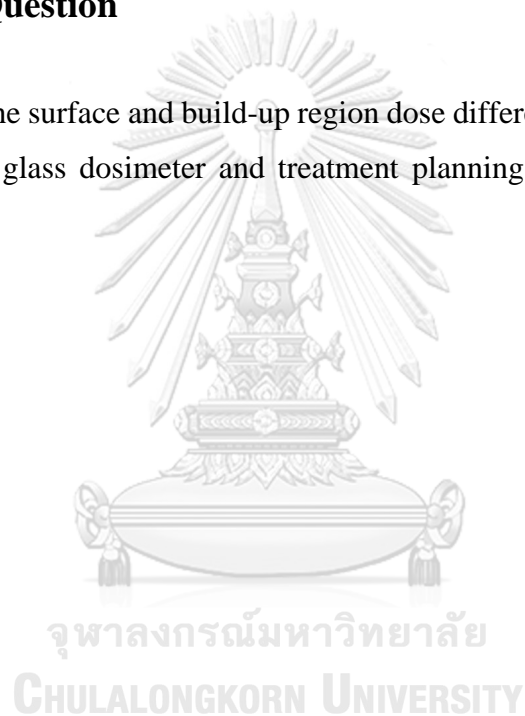
RESEARCH METHODOLOGY

3.1 Research Design

This study is an observational analytical study.

3.2 Research Question

What are the surface and build-up region dose differences between using radio-photoluminescent glass dosimeter and treatment planning system in head and neck region?



3.3 Research Design Model

This study is divided into three main parts, the dosimetric characteristics study, the phantom study and the clinical application. The details of research design model are presented in Fig 3.1.

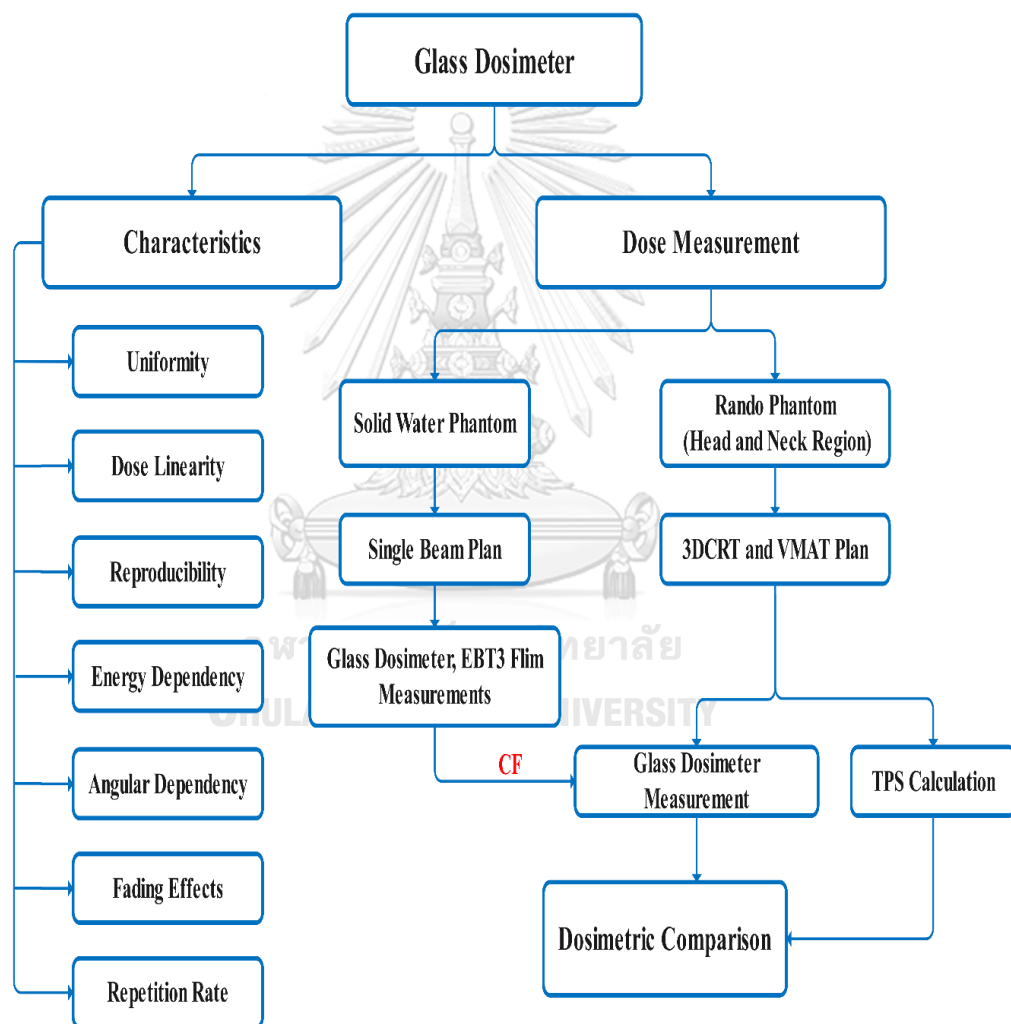


Figure 3.1 Research Design Model.

3.4 Conceptual Framework

The surface dose in radiotherapy is influenced by factors such as the dose calculation algorithm used in TPS, treatment techniques and other factors such as field size and photon energy as presented in Fig 3.2. Moreover, surface dose differs with the dosimeter used to measure it due to different effective points of measurement.

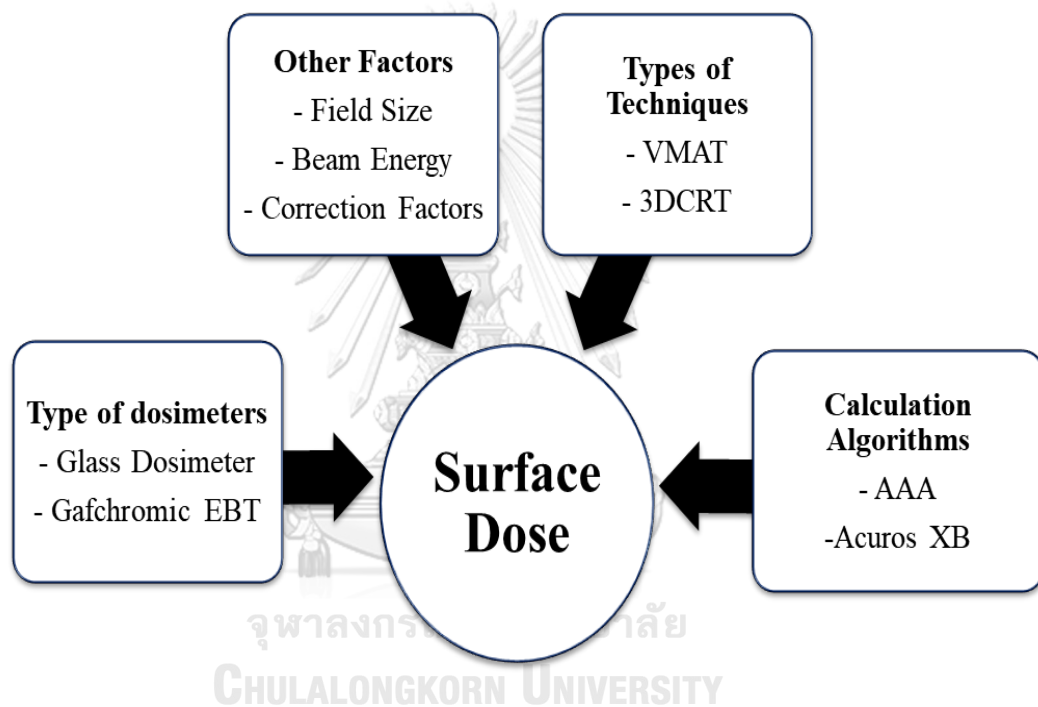


Figure 3.2 Conceptual Framework.

3.5 Materials

The materials used in this study are from the Department of Radiation Oncology, King Chulalongkorn Memorial Hospital.

3.5.1 Varian Clinac iX

The Clinac iX linear accelerators (Varian Medical Systems, Palo Alto, USA) is a linear accelerator that can deliver both high energy x-ray beams at 6 and 10 MV with 120 millennium MLC and 4, 6, 9, 12, 16 and 20 MeV electron beams. The range of field sizes is from $0.5 \times 0.5 \text{ cm}^2$ to $40 \times 40 \text{ cm}^2$ at isocenter. The distance from the target to the isocenter is 100 cm. The dose rates can be adjusted from 100 to 600 MU/min for conventional mode. (Fig 3.3)



Figure 3.3 Varian RapidArc.

CHULALONGKORN UNIVERSITY

3.5.2 Varian Clinac 23EX

The Clinac 23EX (Varian medical systems, Palo Alto, USA) is a linear accelerator that can deliver both high energy x-ray beams at 6 and 15 MV with 120 millennium MLC and 4, 6, 9, 12, 16 and 20 MeV electron beams. The range of field sizes is from $0.5 \times 0.5 \text{ cm}^2$ to $40 \times 40 \text{ cm}^2$ at isocenter. The distance from the target to the isocenter is 100 cm. The dose rates can be adjusted from 100 to 600 MU/min for conventional mode. (Fig 3.4)



Figure 3.4 Varian Clinac 23EX.

3.5.3 Siemens CT Scanner

The 64 slices CT is capable of adapting to virtually every patient and every clinical question. It comes with an ultra-fast ceramic detector with rotation time up to 30 seconds and temporal resolution up to 150 ms. The kV selections can be made from 70, 80, 100, 120 and 140 kV. Fueled by the FAST CARE platform, the SOMATOM Definition AS (Global Siemens Healthcare, Erlangen, Germany) is designed to help maximize clinical outcome and to raise patient-centric productivity. The new SOMATOM Definition AS can be upgraded with the Stellar detector for state-of-the-art signal detection and noise reduction. (Fig 3.5) (31)



Figure 3. 5 Siemens CT Scanner.

3.5.4 Solid Water Phantom

The solid water phantoms (RMI-Gammex, Inc., Middleton, WI, USA) which has the density of 1.02 g/cm^3 , and atomic number of 5.95 is made in square slabs of $30 \times 30 \text{ cm}^2$ with various thickness of 2 mm to 5 cm. (Fig 3.6)



Figure 3. 6 Solid water phantom.

3.5.5 Disk Phantom

Disk phantom (IBA Dosimetry GmbH, Schwarzenbruck, Germany) is used for verification of the isocenter. In this study it was used in angular dependence study of the glass dosimeter. The phantom is made out of poly methyl methacrylate (PMMA) and about weighs about 2 kg. The phantom has a thickness of 20 mm and with 200 mm diameter (Fig 3.7)

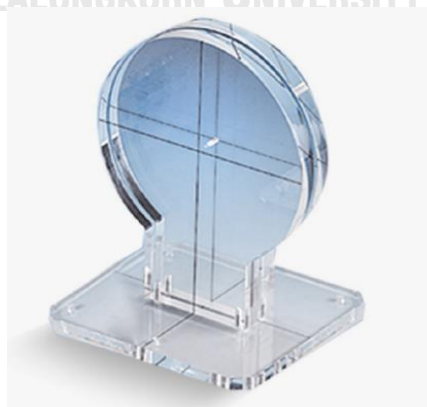


Figure 3. 7 Disk phantom.

3.5.6 Alderson Rando phantom

Alderson Rando phantom (The Phantom Laboratory, Salem, NY, USA) is an anthropomorphic phantom as shown in figure 3.8 and is used to measure dosimetric effect of dosimeters. The rando phantom is transected horizontally into 2.5 cm thick slices. Each slice has holes which are plugged with bone-equivalent, soft tissue equivalent or lung tissue equivalent pins which can be replaced by TLD or glass dosimeter holder pins. The phantom is molded of tissue-equivalent material, which has similar effective atomic number to the body's soft tissue.



Figure 3. 8 Alderson Rando Phantom.

3.5.7 Tissue Mimicking Bolus

In radiation therapy, bolus sheets (Civco Radiotherapy, Orange City, Iowa, USA) are often used when treating uneven areas of a patient, such as at the nose or ears, to make up for missing tissue, or to provide build-up of dose to the skin surface. The bolus made of tissue equivalent material such as synthetic oil gel with a specific gravity of 1.02 g/cm^3 . It is based on vinyl plastic containing a large amount of diisodecyl phthalate. It is 0.5 cm to 1.5 cm thick and 30 cm square shape. (Fig 3.9)

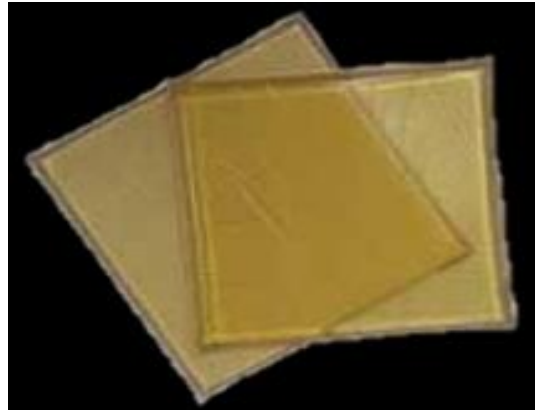


Figure 3. 9 Tissue Mimicking Bolus.

3.5.8 Radio-Photoluminescent Glass Dosimeter (RPLGD)

The glass dosimeter model used in this study was model GD-302M (Chiyoda Technol Dose Ace, Tokyo, Japan) series FD-7. RPLGD uses silver activated phosphate glass as the luminescent material. The shape of this model is cylindrical with 1.5 mm diameter and 12 mm length (without holder) or 2.5 mm diameter with 13 mm (with holder). The density and effective atomic number of glass dosimeter is 2.61 g/cm³ and 12.04, respectively. Before irradiation, the residual signal was removed by an annealing process at 400°C for 1 h using the electric furnace. After irradiation, the luminescent signal was stabilized by the preheat process at 70°C for 30 min. The automatic reader FGD-1000 (AGC Techno Glass Co., LTD, Shizuoka, Japan) was used to readout the signal. (Fig 3.10) (6)



Figure 3. 10 RPLGD 302-M and holder.

3.5.9 Gafchromic EBT3 Film

GAFChromic EBT-3 (Ashland ISP Advanced Materials, NJ, USA) is designed for the measurement of absorbed doses of ionizing radiation. It is particularly suited for high-energy photons. The dynamic range of this film is designed for best performance in the dose range from 0.2 to 10 Gy, making it suitable for many applications in IMRT, VMAT and brachytherapy. For measurement of doses substantially greater than 10 Gy EBT-XD or MDV3 are preferred while the use of HD-V2 is indicated for still higher dose measurement. The size of the EBT3 film is 8" × 10" and other sizes available on request. (Fig 3.11)



Figure 3. 11 Gafchromic EBT3 Film.

3.5.10 Flat-Bed CCD Scanner

The Epson perfection V700 flatbed color CCD (model V700, Epson Seiko Corp., Nagano, Japan) for EBT film digitization is used as a scanner densitometer. The maximum scanning media size is 22×30 cm². The color depth of the scanner is 48-bit color. The optical resolution of scanner is 6400×9600 dpi and the maximum resolution is 12800×12800 dpi of interpolated resolution. It is shown in Fig 3.12.



Figure 3. 12 Epson perfection flat-bed CCD scanner.

3.5.11 Eclipse Treatment Planning System

The Analytical Anisotropic Algorithm (AAA) (Varian Medical System, Inc, Palo Alto, CA, USA) in Eclipse Integrated Treatment Planning, version 15.6 was used in this study. This Eclipse version provides two photon dose calculation algorithms Analytical Anisotropic Algorithm (AAA) and the new algorithm Acuros XB. The new version includes New Varian Service Portal (VSP) to support the Windows Active Directory integration, improved patient chart enhancements, DICOM Export Improvements and options for Varian mobile app that allows access to key features of ARIA (Fig 3.13)

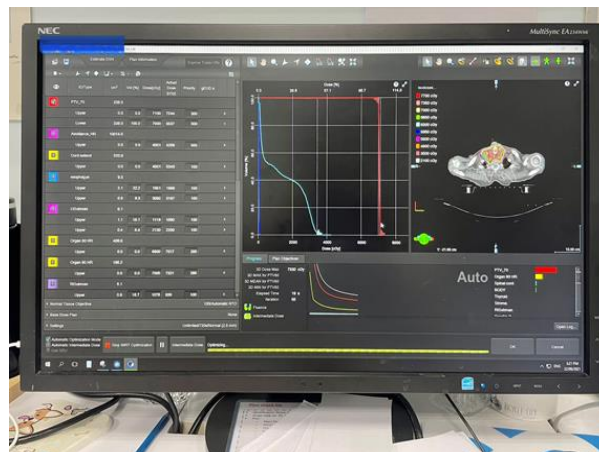


Figure 3. 13 Varian Eclipse TPS.

3.6 Methods

Part 1: Dosimetric Characteristics study of RPLGD

All parts of the study were undertaken on 6-MV photon beams from Varian Clinac iX (Varian Medical System, Palo Alto, CA, USA), except for energy response (used Varian Clinac 23EX for 15 MV) in a homogeneous solid water phantom. The same batch of glass dosimeter was used in this study, which was model GD-302M series FD-7. Before irradiation, the residual signal was removed by an annealing process at 400°C for 1 hour using the electric furnace. After irradiation, the luminescent signal was stabilized by the preheat process at 70°C for 30 minutes. The automatic reader FGD-1000 (AGC Techno Glass Co., LTD, Shizuoka, Japan) was used to readout the signal. Each RPLGD was repeatedly read for five times which was automatically set by FGD-1000 software. The experimental set-up is shown in Fig 3.14.

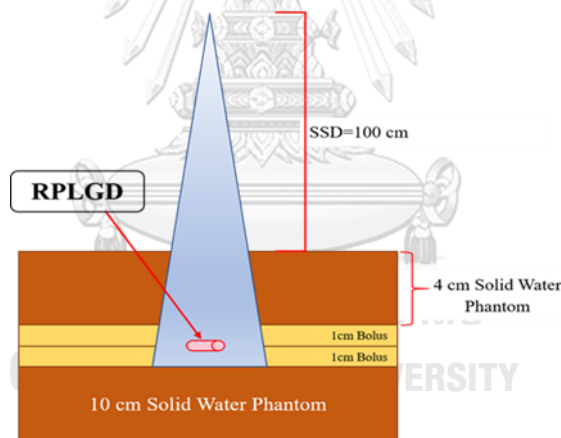


Figure 3. 14 RPLGD set-up for dosimetric characteristics

Uniformity: Twenty-five RPLGDs were exposed to 184 cGy of radiation dose. The batch uniformity of all 25 RPLGDs were determined in relative response, that is the average signal of 5 readouts per RPLGD divided by the average signal for all the 25 RPLGDs.

Reproducibility of Reader: Ten RPLGDs were exposed to 200 cGy of radiation dose. The FGD-1000 reader system was turned on approximately 15 min

before the reproducibility test. For single readout, each RPLGD was re-readout for 5 times. The readout process was run for 3 times on the same day. In each session, the setup of readout magazine was made independently from the previous readout procedure and followed by resetting the FGD-1000 system. Afterward, the readout magazine was pulled in and out to ensure no residual signal was left and affecting the next reading of glass dosimeter.

Linearity: The 40 RPLGDs were investigated to measure various doses at 5, 10, 20, 50, 100, 200, 300 and 500 cGy from 6 MV photon beams (5 GDs each for each of the assigned doses).

Repetition Rate Response: It was performed in 30 RPLGDs (5 each for each rep rate) at 6 MV for 100, 200, 300, 400, 500 and 600 MU/min. The repetition rate response in each step was normalized to 400 MU/min according to our clinical usage.

Energy Response: Thirty RPLGDs were irradiated with similar dose of 200 cGy from 6, 10 and 15 MV photon beams. The average signal response of 10 RPLGDs in each beam quality was normalized to the average signal response of 6 MV.

Angular Dependence: The RPLGD response was examined at gantry angle of 0° to $\pm 90^\circ$ using a disk phantom made from polymethyl-methacrylate (PMMA). The RPLGD was positioned in a perpendicular direction to the incident beam axis into the central hole of the phantom and exposed to fixed 200 MU at a time. Measurements were repeated three times in each gantry angle. The relative response was normalized to the RPLGD readout of the central axis at 0° gantry angle. Each point displays the outcome from average three repeated measurements and five times readout in each RPLGD.

Fading Effect: Forty RPLGDs were exposed to 200 cGy of radiation dose. The glass dosimeters were divided into 10 RPLGDs for readout process for 4 consecutive weeks. The unread RPLGDs were stored in the unexposed radiation area under a room temperature of 25°C . Fading effect was defined as the relative response of glass dosimeter to the initial readout.

Part 2: Surface & build-up region dose measurement in homogeneous solid water phantom using Gafchromic EBT3 film and RPLGD

All the measurements in this part were undertaken on 6 MV photon beams from Varian Clinac iX. The objective of this part of the method was to investigate the feasibility of RPLGD in measuring surface and build-up region dose by comparing with Gafchromic EBT3 film as the reference dosimeter. The experimental conditions as shown in Table 3.1 were kept uniform for both the dosimeters.

All the measurements in this part were undertaken on 6 MV photon beams from Varian Clinac iX. The objective of this part of the method was to investigate the feasibility of RPLGD in measuring surface and build-up region dose by comparing with Gafchromic EBT3 film as the reference dosimeter. The experimental conditions as shown in Table 3.1 were kept uniform for both the dosimeters.

Table 3.1 The experimental conditions in homogeneous solid water phantom

Experimental Conditions	
Field Size	10 × 10 cm ²
Photon Energy	6 MV
Source to Axis	100 cm
MU/min	400
MU	200
Depth	0 (surface), 2, 3, 5 ,10 and 15 mm

Surface and Build-up region dose measurement using EBT3

EBT3 Film Calibration

The EBT3 films were calibrated first at the depth of 1.5 cm in solid water phantom with 10×10 cm² field size, 100 SSD and irradiated with 6 MV photon with

varying dose ranging from 0 to 300 cGy. The experiment set up is shown in Fig 3.15. After that, the films were scanned using a flatbed CCD scanner, 24 hours after irradiation. Then, the signals on the film were read and the calibration curve between the dose and the response signal from the EBT3 films was obtained.

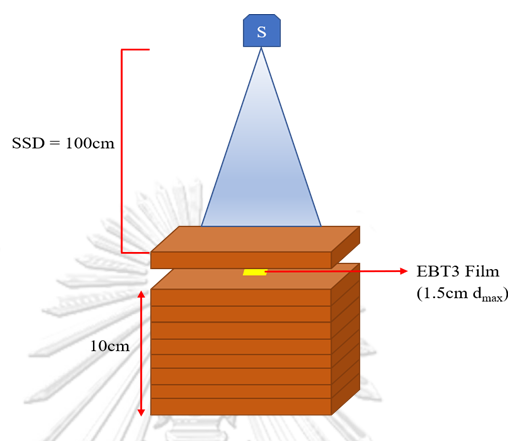


Figure 3. 15 EBT3 film set-up for calibration.

Surface and Build-up region dose measurement using EBT3 film

The EBT film was cut into $20\text{ cm} \times 7\text{ cm}$ dimension. EBT3 was placed vertically as the parallel technique, sandwiched between phantoms. After film was exposed, measurements were done at different depths starting from 0 (surface) to 2, 3, 5, 10 and 15 mm depth. The doses were normalized to the dose at d_{max} . (Fig. 3.16)



Figure 3. 16 EBT3 set-up for dose measurement.

Surface and Build-up region dose measurement using RPLGD

Twenty-five annealed glass dosimeters of model GD-302M series FD-7 were irradiated in groups of 5 glass dosimeters at varying depths from 0 to 2, 3, 5, 10 and 15 mm in a homogeneous solid water phantom. After irradiation, the luminescent signal was stabilized by the preheat process at 70°C for 30 min. The automatic reader FGD-1000 was used to readout the signal. The doses were normalized to the dose at d_{\max} . (Fig 3.17)

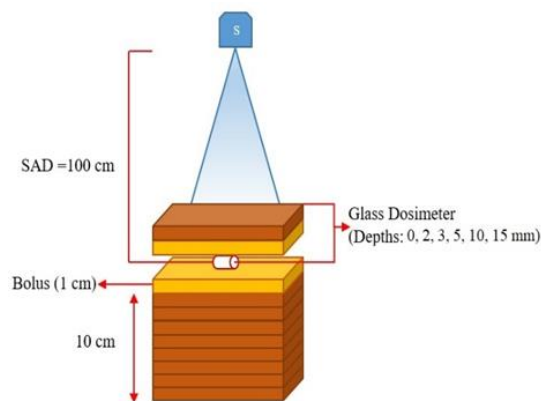


Figure 3. 17 RPLGD set-up for dose measurement.

Part 3: Verification of Plans in H&N Rando Phantom using RPLGD

CT planning of Alderson rando phantom was performed using Siemens SOMATOM Definition AS scanner. (Fig 3.18) CT data were acquired for 3 mm slice thickness with Head and Neck protocol. The acquired CT images were exported to the Varian Eclipse treatment planning system (TPS) via the data networking. The target volume of head and neck region, the clinical target volume (CTV), planning target volume (PTV) and critical structures were created on the CT images. The plans with two treatment techniques for 6 MV photon beams were then undertaken in the TPS for AAA. The two treatment techniques were:

1. 3D-Conformal radiotherapy – 2 Fields, 3 Fields, 4 Fields
2. Volumetric modulated arc therapy (VMAT), three arc beams – 3 cases

For the plan verification, each glass dosimeter was placed on the right maxilla at the level of head & neck region of the rando phantom. (Fig 3.19) Irradiation was performed with the two treatment techniques using Varian Clinac iX and the dose was calculated with AAA. Doses were measured and calculated at the depth of 5 and 10 mm by placing tissue mimicking bolus over the dosimeter at the area of irradiation.

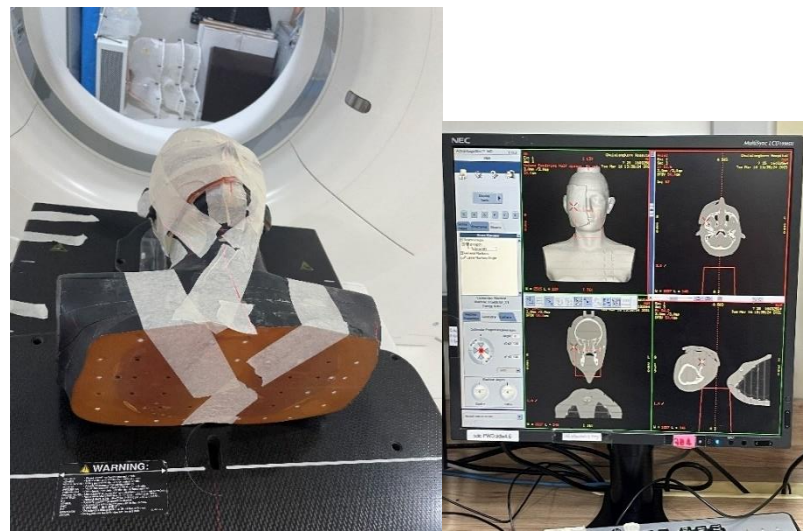


Figure 3. 18 CT scanning of rando phantom; (a) phantom set-up inside CT machine, (b) CT console.

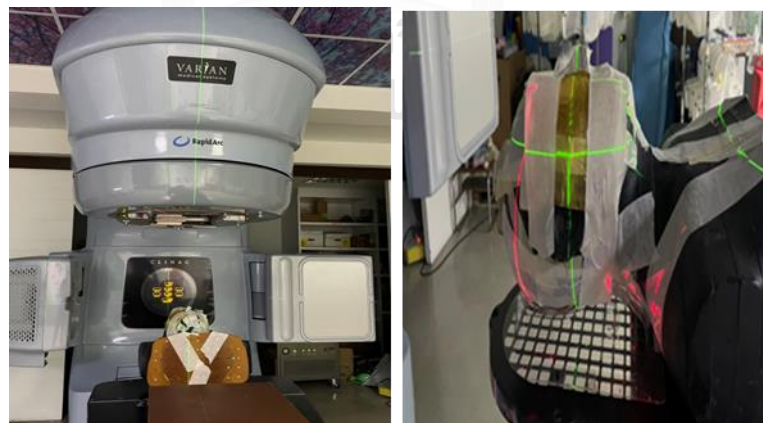


Figure 3. 19 (a) Rando phantom set-up in the treatment machine, (b) placement position of RPLGD on the right maxilla.

3.7 Patient Analysis

The 3 VMAT cases of nasopharyngeal cancer treated with radiation at the Radiation Oncology Division, King Chulalongkorn Memorial Hospital, Bangkok, Thailand were randomly selected. The plans were exported to Rando phantom and the VMAT plans were recalculated. In case of 3D-CRT, 2-field, 3-field and 4-field were created on Rando phantom. The build-up region doses from Eclipse TPS were recorded at 5 mm and 10 mm depth on the right side of phantom and then the calculated doses of AAA were compared with the measured values from RPLGD. (Fig 3.20)

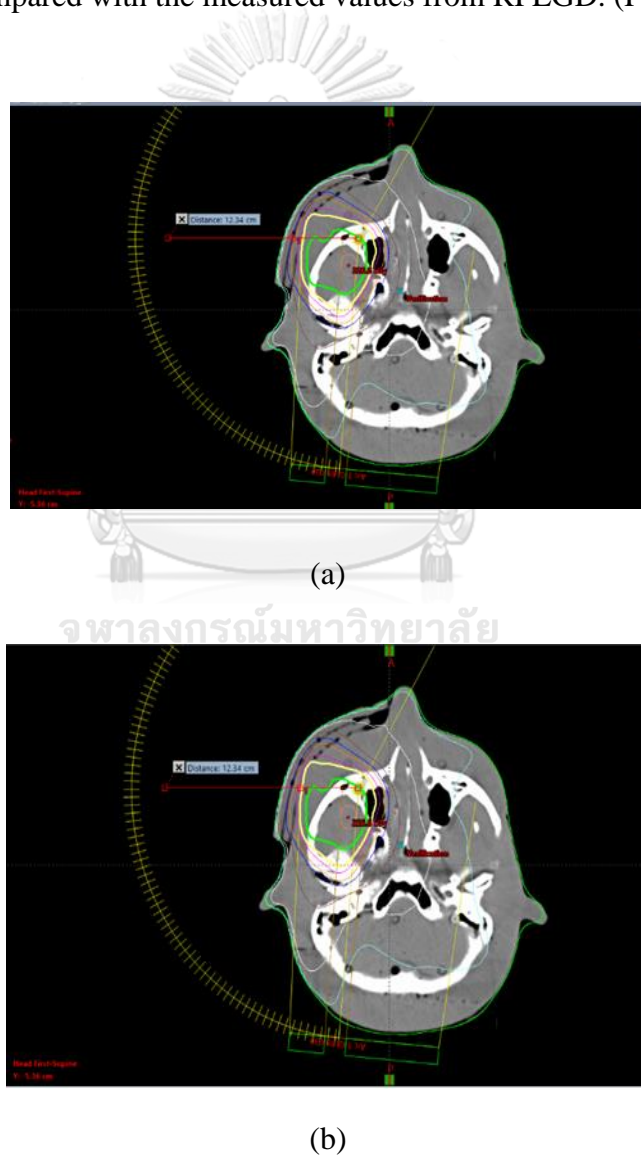


Figure 3. 20 The calculated doses recorded for VMAT; (a) 5 mm, (b) 10 mm.

3.8 Outcome Measurements

The outcomes for surface and build-up region dose measurement and calculation are:

- Percent difference of dose measured between glass dosimeter and gafchromic EBT3 films
- Percent difference of dose between calculated dose in AAA and measured dose using glass dosimeter for the clinical cases of nasopharyngeal cancer with 3DCRT and VMAT techniques.
- Mean and Standard deviation of dosimetric characteristics of glass dosimeter GD-302M

3.9 Sample Size

Sample size was determined such that the mean difference between calculated surface dose from Eclipse Treatment Planning System (AAA) and the measured dose using film dosimeter for VMAT technique was at least 8.38 cGy (variance of the difference = 25.27) with 95% Confidence Interval by using the following equation:

$$n = \frac{(z_{\alpha/2} + z_{\beta})^2}{d^2} \times \sigma^2$$

$$n = 3.77 \approx 6 \text{ cases}$$

where, z is the reliability coefficient of normal distribution

$$\alpha = 0.05, z_{\alpha/2} = 1.96$$

$$\beta = 0.10, z_{\beta} = 1.2816$$

$$\sigma^2 = \text{variance of difference} = 25.27 \text{ [Akbas et al. 2018(32)]}$$

$$d = \text{difference of mean} = 8.38$$

3.10 Statistical Analysis

The dosimetric characteristics of glass dosimeters were expressed in percentage, standard deviation and range and presented in the form of tables and graphs.

The percent difference of dose between calculated dose in AAA and measured dose using glass dosimeter were presented in the form of tables and graphs.

3.11 Expected Benefit

This study was helpful in determining the suitability of using Radio photoluminescence glass dosimeter in surface and build-up region dose measurement in radiotherapy and its feasibility as in-vivo dosimeter.

3.12 Ethical Consideration

Although this study was performed in phantom, retrospective cases were randomly collected from the ARIA database system from the Radiation Oncology Division, King Chulalongkorn Memorial Hospital. Therefore, the research proposal was submitted for ethical consideration and was approved by the Ethics Committee of the Faculty of Medicine, Chulalongkorn University. (Fig 3.21)





 COA No. 955/2020 IRB No. 428/63 INSTITUTIONAL REVIEW BOARD Faculty of Medicine, Chulalongkorn University 1873 Rama 4 Road, Patumwan, Bangkok 10330, Thailand, Tel. 662-256-4493	 Dr. Taweap Sanghathum, Ph.D. Signature  (Emeritus Professor Tada Sueblinwong MD) Chairperson The Institutional Review Board
Certificate of Approval The Institutional Review Board of the Faculty of Medicine, Chulalongkorn University, Bangkok, Thailand, has approved the following study which is to be carried out in compliance with the international guidelines for human research protection as Declaration of Helsinki, The Belmont Report, CIOMS Guideline and International Conference on Harmonization in Good Clinical Practice (ICH-GCP)	
Study Title : Surface and build-up region dose measurement in head and neck region using radio-photoluminescent glass dosimeter	Signature  (Associate Professor Suprecha Wittayaleertpanya) Member and Assistant Secretary, Acting Secretary The Institutional Review Board
Study Code : -	Date of Approval : August 1, 2020 Approval Expires Date : July 31, 2021
Principal Investigator : Miss Soram Choki	
Affiliation of PI : Department of Radiology, Faculty of Medicine, Chulalongkorn University.	
Review Method : Expedited	
Continuing Report : At least once annually or submit the final report if finished.	
Document Reviewed : <ol style="list-style-type: none"> 1. Research Proposal Version 2.0 Date 7th July 2020 2. Protocol Synopsis Version 2.0 Date 7th July 2020 3. Case Record Form Version 1.0 Date 13th May 2020 4. Curriculum Vitae and GCP Training <ul style="list-style-type: none"> - Miss Soram Choki 	
Approval granted is subject to the following conditions: (see back of this Certificate)	

Figure 3. 21 Certificate of approval by Ethics Committee of the Faculty of Medicine, Chulalongkorn University.



CHAPTER 4 RESULTS

4.1 Dosimetric Characteristics of RPLGD

4.1.1 Uniformity

The uniformity reading from 25 RPLGDs is presented in graph. (Fig 4.1) Our study found the uniformity was within $\pm 1.1\%$.

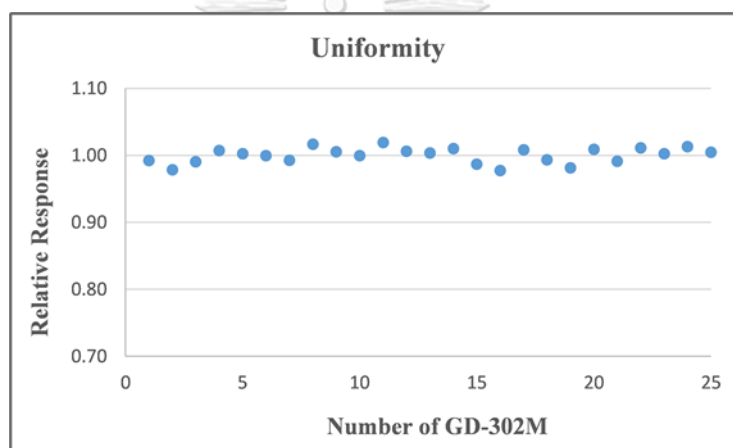


Figure 4. 1 The uniformity of 25 RPLGDs for 6-MV photon beams. The readout for each RPLGD was normalized to the average readout of 25 RPLGDs.

CHULALONGKORN UNIVERSITY

4.1.2 Reproducibility of the dosimeter reader

The reproducibility of FDG-1000 reader system was explored in 10 RPLGDs for three times. The reproducibility was expressed as coefficient of variation in percentage and the value we found was within $\pm 0.9\%$ on an average. (Fig.4.2)

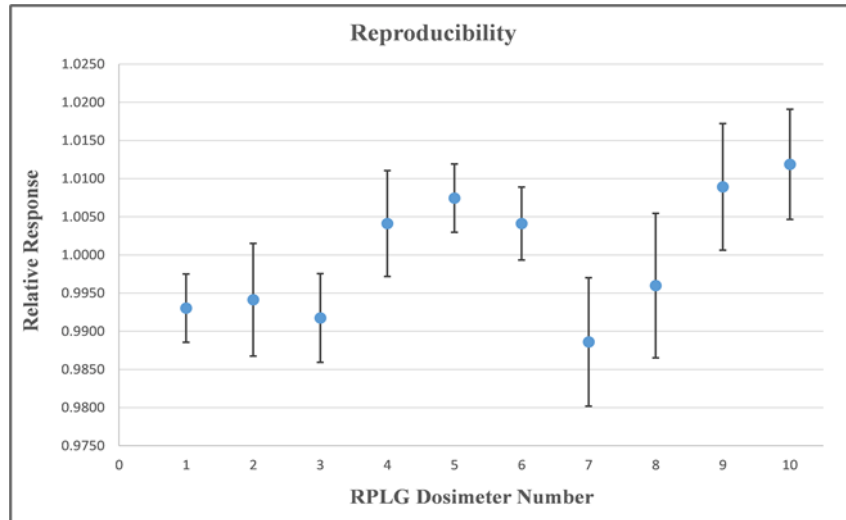


Figure 4. 2 The relative response of FDG-1000 reader system from 10 RPLGDs.

4.1.3 Linearity

As shown in Figure 4.3, the response of RPLGD yielded a linear response between delivered and signal response with coefficient of determination; R^2 of 0.9998.

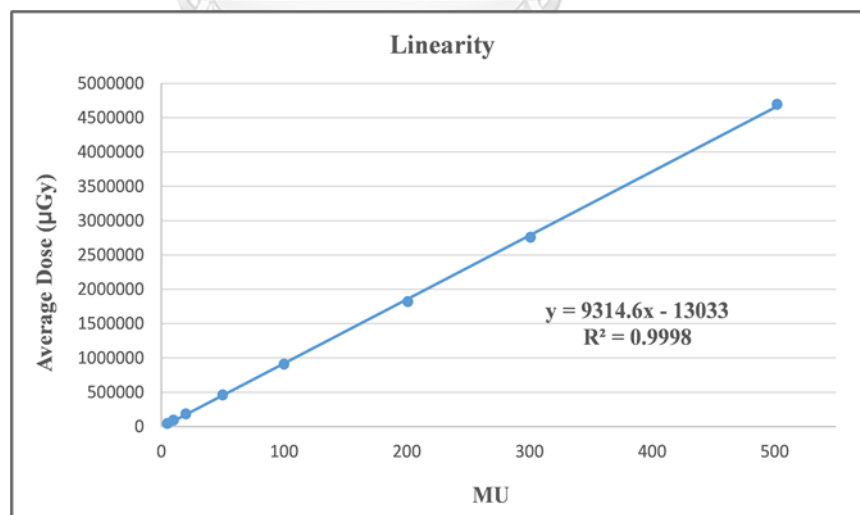


Figure 4. 3 The linearity response of RPLGD.

4.1.4 Repetition Rate Response

The repetition rate response in each step was normalized to 400 MU/min according to clinical usage. The repetition rate is as depicted in the Fig 4.4. The error bars demonstrate the standard deviation over 5 RPLGDs. The maximum error of relative response to 400 MU/min was 1.029 ± 0.005 at 100 MU/min repetition rate.

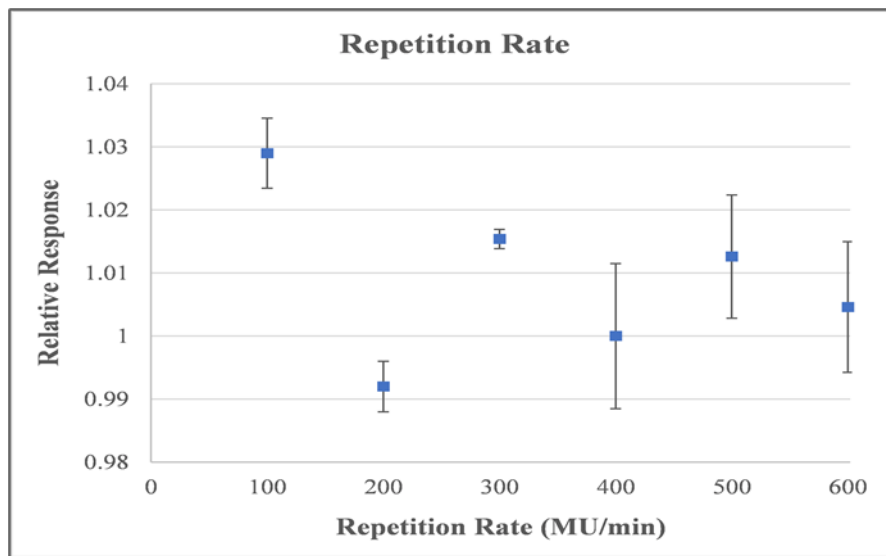


Figure 4. 4 The Rep. rate response of RPLGD.

4.1.5 Energy Response

Table 4.1 summarizes the energy response of RPLGD from various high-energy photon beams relative to 6 MV photon beams. The maximum relative response was 0.977 ± 0.011 for 15 MV.

Table 4.1 Energy response of RPLGD

Energy (MV)	Relative Response to 6 MV
6 MV	1.000 ± 0.011
10 MV	0.982 ± 0.013
15 MV	0.977 ± 0.011

4.1.6 Angular Dependence

As shown in figure 4.5, the relative response of RPLGD across $\pm 90^\circ$ gantry angles was less than or equal to 2%.

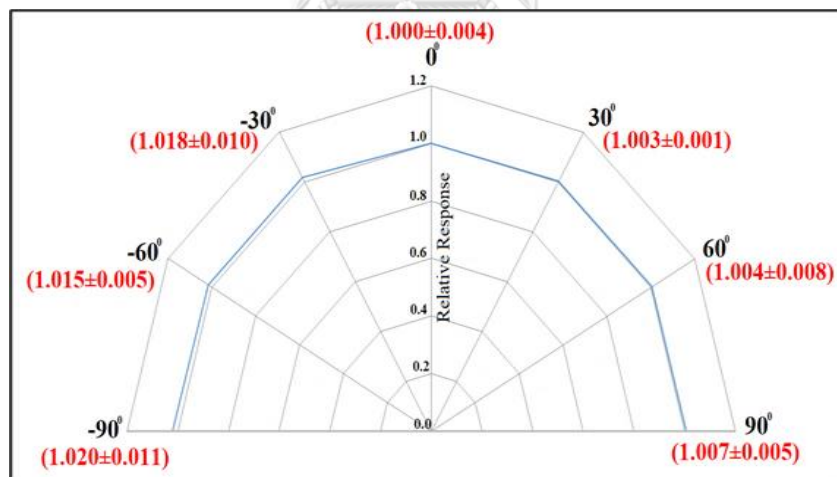


Figure 4. 5 The angular dependence of RPLGD at various gantry angles.

4.1.7 Fading Effect

The fading effect was observed for 4 consecutive weeks. The range of relative response to the first read-out was from 0.974 to 1.000 as shown in figure 4.6, showing negligible fading effect, especially after 3 weeks.

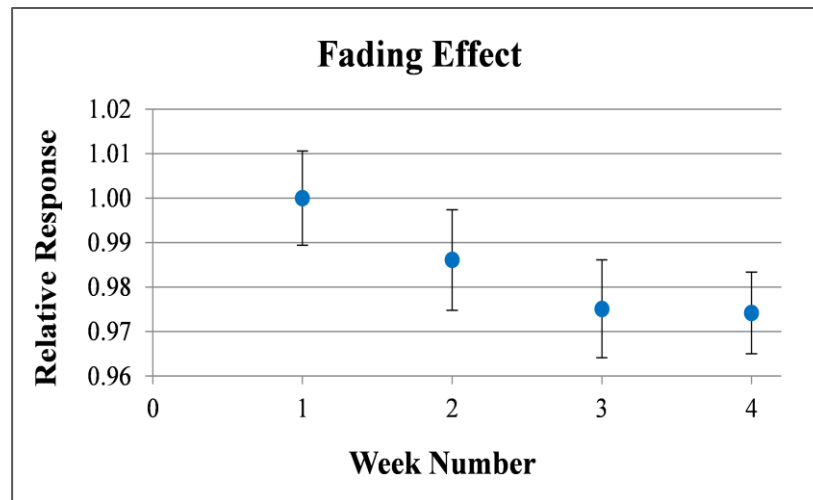


Figure 4. 6 The fading response of RPLGD.

4.2 EBT3 Calibration

The calibration curve was used for film measurement reading. It showed an exponential shape. (Fig 4.7)

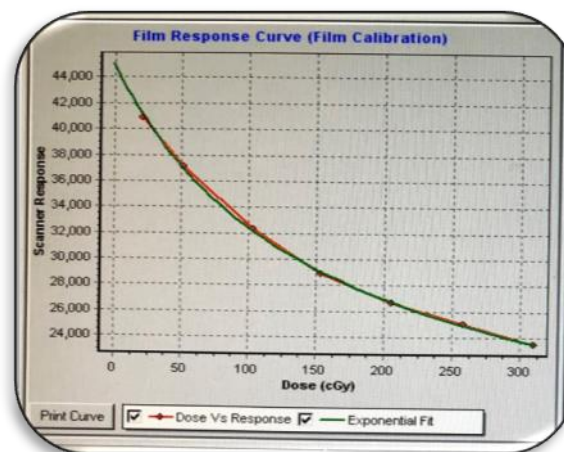


Figure 4. 7 Film calibration curve.

4.3 Surface & Build-up Region Doses in Homogeneous Solid Water Phantom

Taking EBT3 film as the reference dosimeter, the comparison of surface and build-up region doses with the RPLGD and EBT3 in the homogeneous solid water slab phantom are shown in the Table 4.2 and Fig 4.8. The measured doses were expressed as percentage of maximum dose at depth for 6 MV photon energy. The percentage depth dose (PDD) measured at the surface (0 mm depth) with EBT3 was accounted for its effective point of measurement depth of 0.153 mm. A correction factor of 0.854 necessary to scale the dose measured at the effective point of measurement was applied to obtain an accurate skin dose estimate at the clinically relevant depth for EBT3 measurement. After applying the correction factor, the PDD at the surface decreased from 31.14% to 26.59% for EBT3. The percentage depth dose (PDD) measured at the surface (0 mm depth) with RPLGD was comparatively higher than the film measurement with 63.02%. The percent difference between the RPLGD and EBT3 at the surface was 137 %. Below the surface, the percent differences between RPLGD and EBT3 film reduced. The percent difference was calculated using this equation:

$$\% \text{ difference} = \frac{\text{glass reading} - \text{film reading}}{\text{film reading}} \times 100$$

Table 4.2 Surface & Build-up Region Dose comparison between EBT3 and RPLGD in solid water phantom.

Depths	Dose (%)		Dose Difference (%)
	RPLGD	EBT3	EBT3 & RPLGD
Surface	63.02	26.59	137.00
2 mm	80.95	72.46	11.71
3 mm	86.53	80.56	7.41
5 mm	93.98	89.74	4.72
10 mm	98.26	99.39	-1.13
15 mm	100.00	100.00	0.00

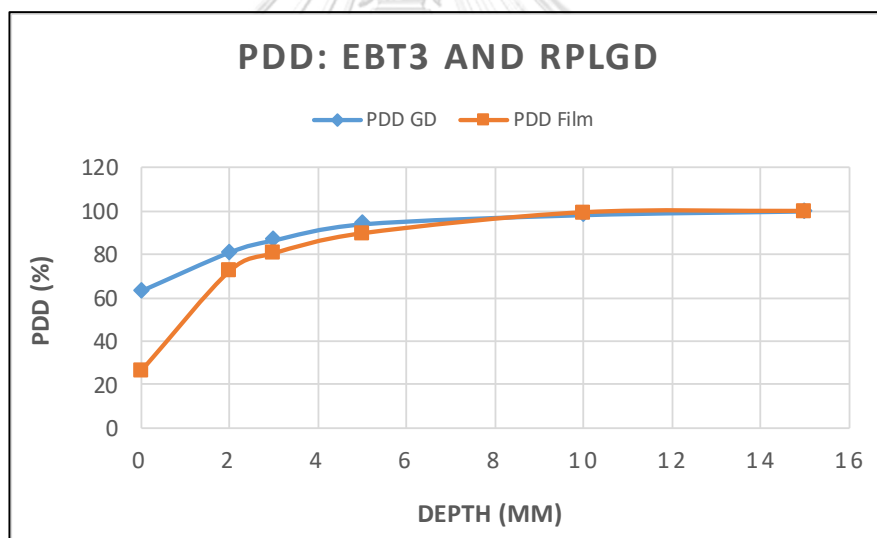


Figure 4. 8 Surface & Build-up Region Dose comparison between EBT3 and RPLGD in solid water phantom.

4.4 Verification of Plans in H&N Rando Phantom using RPLGD

The RPLGD measurement of the two treatment techniques for AAA at build-up region are shown in figure 4.9 and figure 4.10. In these graphs both techniques demonstrated the same pattern. The calculated doses in treatment planning system (TPS) using AAA was found to be higher than the measured doses with RPLGD for both techniques. In 3DCRT technique, the mean percent difference between TPS and RPLGD was found to be $-0.80 \pm 1.21\%$ and $2.40 \pm 1.49\%$ at 5 mm and 10 mm depths, respectively. The mean percent difference between AAA and RPLGD in VMAT was found to be $4.74 \pm 1.12\%$ and $3.44 \pm 4.41\%$ at 5 mm and 10 mm depths, respectively as shown in Table 4.3. The VAMT technique illustrated higher dose than the 3DCRT technique at both depths with mean percent difference of 4.63% and 7.71% with RPLGD and TPS, respectively. Moreover, in 3D-CRT, 2-field technique showed more dose percent difference between TPS and RPLGD than 3 and 4-field box techniques.

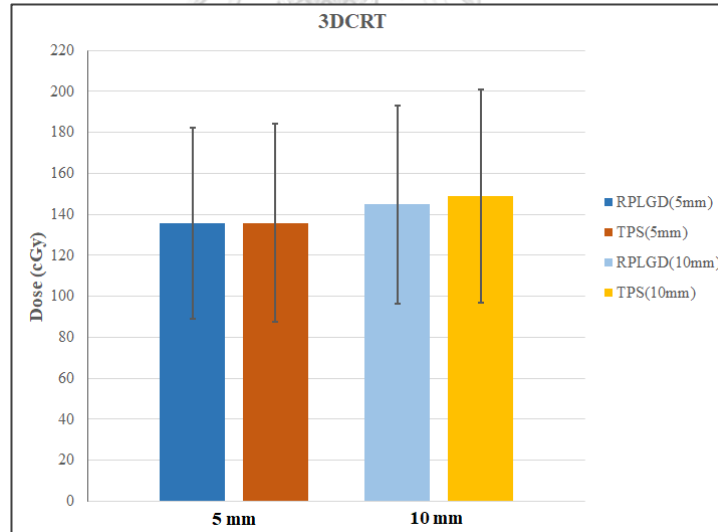


Figure 4. 9 Build-up dose measurement and calculation for 3D-CRT.

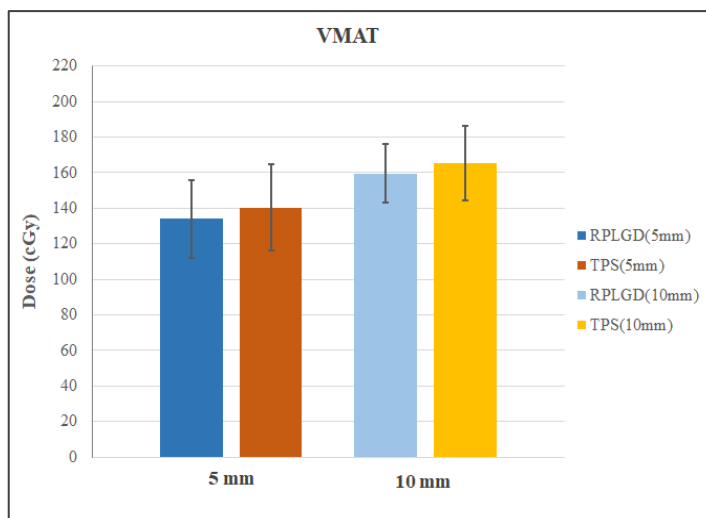


Figure 4.10 Build-up dose measurement and calculation for VMAT.

Table 4.3 Build-up dose comparison between TPS (AAA) and RPLGD

Techniques	Eclipse TPS (cGy)		RPLGD (cGy)		Dose Difference (%)	
	5 mm	10 mm	5 mm	10 mm	5 mm	10 mm
3DCRT 2F	189.6	206.5	187.5	198.3	1.08	4.12
3DCRT 3F	122.0	134.0	122.3	131.7	-0.29	1.67
3DCRT 4F	95.7	105.8	97.0	104.3	-1.34	1.42
	Mean Differences ±SD				-0.18±1.21%	2.40±1.49%
VMAT 1	117.9	142.0	113.8	143.3	3.50	-0.93
VMAT 2	137.5	171.3	130.8	158.7	5.06	7.88
VMAT 3	166.0	182.5	157.0	176.5	5.67	3.38
	Mean Differences ±SD				4.74±1.12%	3.44±4.41%

CHAPTER 5

DISCUSSION AND CONCLUSION

5.1 Discussion

Accurate knowledge of surface and build-up doses is important especially in cases where the skin acts as the dose limiting tissue. But the measurement of surface and build-up region dose is a challenging issue shared in many publications and it is further challenged with the need of a dosimeter with an appropriate physical property to measure the surface dose accurately. Moreover, TPS calculations cannot be accurate especially in the surface and build-up region due to lack of electronic equilibrium in this region. An extrapolation chamber is considered the most ideal dosimeter for surface dose measurement but it is not practical to use in a hospital. The physical characteristics of RPLGD are reported to be better than that of OSLD and TLD because of different readout system and different luminescence material. Therefore, in this study, the feasibility of RPLGD was evaluated by comparing it with Gafchromic EBT3 film, which is a new type of Gafchromic film model. EBT3 was used as a reference dosimeter in this study mainly because of its high spatial resolution and low spectral sensitivity, make them ideal for the measurement of dose distributions in regions of a high dose gradient in radiation fields.(16)

5.1.1 Dosimetric Characteristics of RPLGD

In our study, RPLGD showed good uniformity of 1.1% (1 SD) and good linear response with R^2 of 0.999. This agreed well with the result from Oonsiri, P., et al. (33) and Son, K., et.al.(34) The reader reproducibility result was also in agreement with that from Oonsiri, P., et al. with relative response of $\pm 0.5\%$ which indicated that the FGD-1000 reader system was very stable.(33) Dose rate, reproducibility, angular and energy dependence were found to be within 3.0%. The energy dependent effect was less but it increased with energy because for un-filtered GD-302M, photoelectric effect decreases

with higher photon energy as shared by Huang, D., et al. in his study. (6) Moreover, fading effect was less than 3% over 4 weeks.

5.1.2 Surface and Build-up region Dose Measurement

In this study surface and build-up region doses were compared between RPLGD and EBT3 film in solid water phantom at 0, 2, 3, 5, 10 and 15 mm depths of 6 MV beams. The effective point of measurement for EBT3 was taken into consideration when correcting for surface dose. The effective point of measurement for EBT3 was defined at 0.153 mm depth for surface dose measurement in the study by Akbas, U., et al. (5) Our result with EBT3 film for surface dose was found to be 26.59%. Akbas, U., et al. in their study showed 20.4% using EBT3 film at the depth of 0 mm for 10×10 cm² field size. Qi, Z.Y., et al. (35) also searched for surface dose with an EBT film at the phantom surface where the effective measurement depth equals 0.153 mm and the result was 23.5%. Bilge, H., et al. (36) used EBT film and measured the surface dose equal to $20.0 \pm 2\%$. Our EBT3 film results for surface and build-up dose measurement showed good agreement with other publications. However, our result with RPLGD for surface dose was found to be 63.02%, which showed a very large difference compared to our reference EBT3 dosimeter. It appears there is an over-response of signal at the surface with RPLGD. The reason may be attributed to the physical property of RPLGD. The RPLGD has a diameter of 1.5 mm (without holder) & 2.5 mm (with holder). In this study, doses were measured with the holder, which acts as a build-up material and although surface dose is measured at an infinitesimally small effective area, the depth measured is not the true surface (little above surface). Consequently, a very large correction factor is required to scale it down but a large correction factor as required in this study does not seem appropriate. Determining the appropriate correction factor for surface dose in this case can most likely be accomplished through detailed Monte Carlo work. This makes RPLGD less feasible to measure at the surface with the requirement of very large correction factor. However, in the build-up region, the PDD measured values agreed well between RPLGD and EBT3.

5.1.3 Verification of Plans in Rando Phantom with RPLGD

Observing that RPLGD is less feasible to measure surface dose, dose verification for 3DCRT and VMAT plans in AAA were carried out in the build-up region at depths of 5 mm and 10 mm. In 3DCRT, the field-in-field technique was used with 2, 3 and 4 fields, which was then averaged for comparison. The results obtained from RPLGD measurements were found to be lower in both techniques compared with TPS calculations with an average difference of 1.1% for 3DCRT and 4.0% for VMAT. Although, equal prescribed dose of 200 cGy to the PTV was given, the VMAT technique recorded higher dose than the 3DCRT technique at both depths with mean percent difference of 4.63% and 7.71% using RPLGD and TPS calculation, respectively. This is because in VMAT, there is delivery of radiation from a continuous rotation of the radiation source and allows the glass dosimeter to be irradiated from all angles. In addition to using a larger monitor units (MU) compared with conventional CRT plans, the intensity modulated beam technique in VMAT can also deliver highly conformal dose distributions to the target structures. On the other hand, 3DCRT technique gives uniform dose distribution with high level of precision and accuracy to the area of interest. It is recommended in tumors that are close to vital organs such as in head and neck tumors. In our study, for the 3DCRT, 2-field technique showed more percent dose difference between AAA and RPLGD than 3 and 4-field box techniques. This is because in 2 field technique, the gantry is rotated within two different angles and hence, the radiation across the glass dosimeter varied. Moreover, in 2 field technique, two 45° wedges were used to achieve a trapezoid shaped high dose region. This technique is useful in relatively low-lying lesions (e.g., maxillary sinus and thyroid lesions). (17)

The percent differences between the calculated and measured doses at depths of 5 mm and 10 mm for both the techniques were all found to be within the IAEA TRS430 (37) tolerance that allowed up to 20% dose difference between calculated and measured doses in the build-up region.

5.2 Conclusion

After the evaluation of the dosimetric characteristics of RPLGD and with its small volume, it has prospective potential to be used as an in-vivo dosimeter in high energy photon beam in radiotherapy. Although glass dosimeter has been found to have less feasibility for surface dose measurement, but there are rooms for further study to investigate it further. In head and neck cancer patient treatment, higher doses to the target volumes can be delivered using intensity-modulated techniques such as VMAT and moreover 2-field technique can be useful in relatively low-lying lesions in maxillary sinus. Although there are discrepancies in the measured dose using RPLGD and calculated dose in TPS in the build-up region, the overestimation and underestimation should be carefully considered. The surface and buildup region doses should be evaluated considering the effective measurement depths of dosimeters, which if not considered can vary the results of the measurements.

APPENDIX

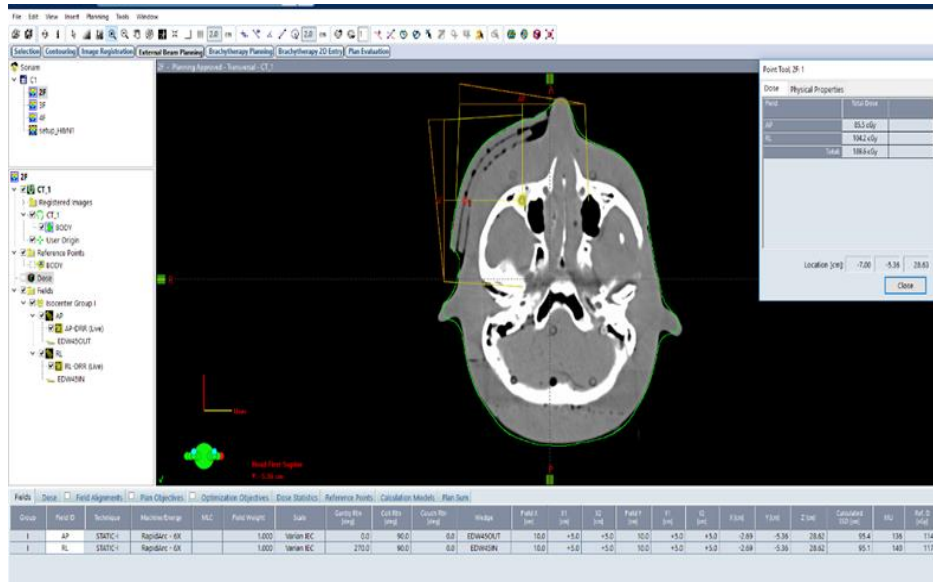


Figure I. 2F-3DCRT plan of rando phantom



Figure II. 3F-3DCRT plan of rando phantom

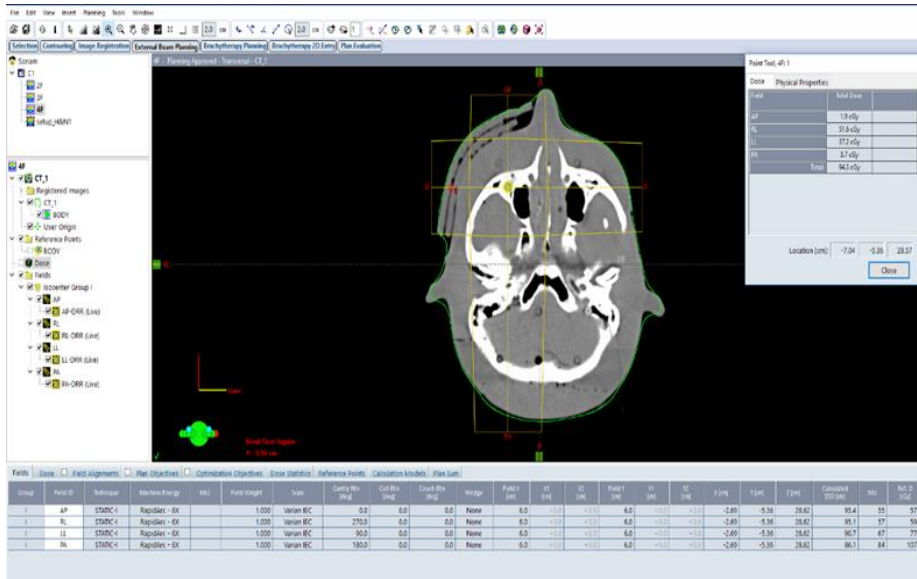


Figure III. 4F-3DCRT plan of rando phantom

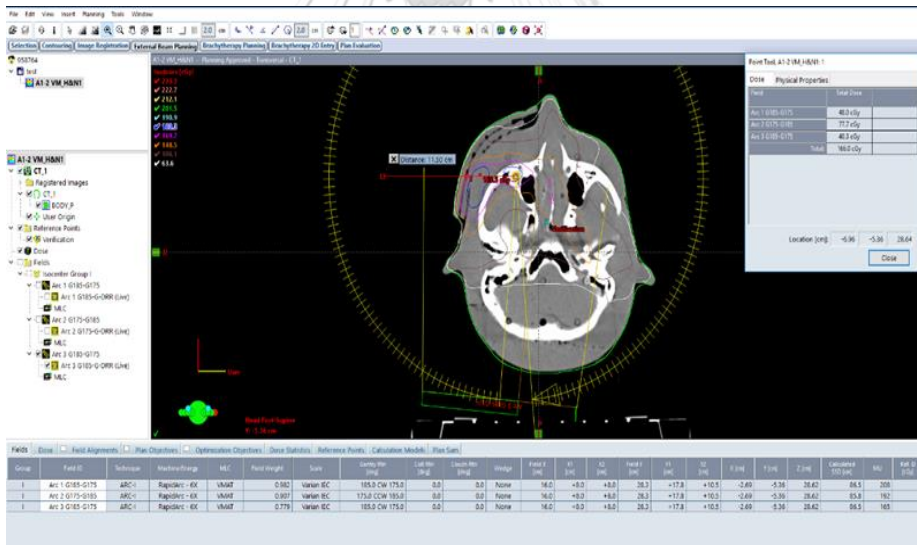


Figure IV. VMAT case no. 1 plan of rando phantom

REFERENCES

1. Sixel KE, Podgorsak EB. Buildup region and depth of dose maximum of megavoltage x-ray beams. *Med Phys.* 1994;21(3):411-6.
2. Nilsson B, Brahme A. Electron contamination from photon beam collimators. *Radiother Oncol.* 1986;5(3):235-44.
3. Petti PL, Goodman MS, Sisterson JM, Biggs PJ, Gabriel TA, Mohan R. Sources of electron contamination for the Clinac-35 25-MV photon beam. *Med Phys.* 1983;10(6):856-61.
4. Kry SF, Smith SA, Weathers R, Stovall M. Skin dose during radiotherapy: a summary and general estimation technique. *J Appl Clin Med Phys.* 2012;13(3):3734-.
5. Akbas U, Donmez Kesen N, Koksal C, Bilge H. Surface and Buildup Region Dose Measurements with Markus Parallel-Plate Ionization Chamber, GafChromic EBT3 Film, and MOSFET Detector for High-Energy Photon Beams. *Advances in High Energy Physics.* 2016;2016:8361028.
6. Huang D, Hsu S-M. Radio-Photoluminescence Glass Dosimeter (RPLGD). 2011.
7. Rah J-E, Hwang U-J, Jeong H, Lee S-Y, Lee D-H, Shin DH, et al. Clinical application of glass dosimeter for in vivo dose measurements of total body irradiation treatment technique. *Radiation Measurements.* 2011;46(1):40-5.
8. Butson M, Yu P, Cheung T, Metcalfe P. Radiochromic film for medical radiation dosimetry. *Materials Science & Engineering R-reports - MAT SCI ENG R.* 2003;41.
9. McLaughlin WL, Miller A, Fidan S, Pejtersen K, Batsberg Pedersen W. Radiochromic plastic films for accurate measurement of radiation absorbed dose and dose distributions. *Radiation Physics and Chemistry (1977).* 1977;10(2):119-27.
10. Board CNE. Head and Neck Cancer: Introduction 2019 [Available from: <https://www.cancer.net/cancer-types/head-and-neck-cancer/introduction>].
11. Ministry of Public Health T. Hospital-Based Cancer Registry 2016 2016 [Available from: https://www.nci.go.th/th/File_download/Nci%20Cancer%20Registry/Hospital-Based%20NCI2%202016%20Web.pdf].

12. Naiyanet N, Oonsiri S, Lertbutsayanukul C, Suriyapee S. Measurements of patient's setup variation in intensity-modulated radiation therapy of head and neck cancer using electronic portal imaging device. *Biomed Imaging Interv J.* 2007;3(1):e30-e.
13. Khan FM, Gibbons JP. Khan's the physics of radiation therapy. Fifth edition ed. Philadelphia, PA: Lippincott Williams & Wilkins/Wolters Kluwer; 2014 2014. 572 p.
14. Herrassi MY, Bentayeb F, Malisan MR. Comparative study of four advanced 3d-conformal radiation therapy treatment planning techniques for head and neck cancer. *J Med Phys.* 2013;38(2):98-105.
15. Otto K. Volumetric modulated arc therapy: IMRT in a single gantry arc. *Med Phys.* 2008;35(1):310-7.
16. Devic S, Seuntjens J, Abdel-Rahman W, Evans M, Olivares M, Podgorsak EB, et al. Accurate skin dose measurements using radiochromic film in clinical applications. *Med Phys.* 2006;33(4):1116-24.
17. Podgorsak EB. *Radiation Oncology Physics: A handbook for Teachers and Students.* Editor T, editor. Vienna2005.
18. Jin H, Palta J, Suh TS, Kim S. A generalized a priori dose uncertainty model of IMRT delivery. *Med Phys.* 2008;35(3):982-96.
19. Lee N, Chuang C, Quivey JM, Phillips TL, Akazawa P, Verhey LJ, et al. Skin toxicity due to intensity-modulated radiotherapy for head-and-neck carcinoma. *International journal of radiation oncology, biology, physics.* 2002;53(3):630-7.
20. Fraass B, Doppke K, Hunt M, Kutcher G, Starkschall G, Stern R, et al. American Association of Physicists in Medicine Radiation Therapy Committee Task Group 53: quality assurance for clinical radiotherapy treatment planning. *Med Phys.* 1998;25(10):1773-829.
21. Kinkhikar RA, Murthy V, Goel V, Tambe CM, Dhote DS, Deshpande DD. Skin dose measurements using MOSFET and TLD for head and neck patients treated with tomotherapy. *Appl Radiat Isot.* 2009;67(9):1683-5.
22. Yorke E AR, Ding L, et al. . Diode In Vivo Dosimetry for Patients Receiving External Beam Radiation Therapy: Report of Task Group 62 of the AAPM Radiation Therapy Committee AAPM Report 87. 2005.

23. Cheung T, Butson MJ, Yu PK. Multilayer Gafchromic film detectors for breast skin dose determination in vivo. *Phys Med Biol.* 2002;47(2):N31-7.
24. Chiu-Tsao ST, Chan MF. Evaluation of two-dimensional bolus effect of immobilization/support devices on skin doses: a radiochromic EBT film dosimetry study in phantom. *Med Phys.* 2010;37(7):3611-20.
25. Eyadeh MM, Wierzbicki M, Diamond KR. Measurement of skin surface dose distributions in radiation therapy using poly(vinyl alcohol) cryogel dosimeters. *J Appl Clin Med Phys.* 2017;18(3):153-62.
26. Nakano M, Hill RF, Whitaker M, Kim JH, Kuncic Z. A study of surface dosimetry for breast cancer radiotherapy treatments using Gafchromic EBT2 film. *J Appl Clin Med Phys.* 2012;13(3):3727.
27. Gibbons JP, Antolak JA, Followill DS, Huq MS, Klein EE, Lam KL, et al. Monitor unit calculations for external photon and electron beams: Report of the AAPM Therapy Physics Committee Task Group No. 71. *Med Phys.* 2014;41(3):031501.
28. Janne Sievinen WUaKW. AAA Photon Dose Calculation Model in Eclipse™.
29. Gafchromic. GAFChromic™EBT3film specifications [Available from: www.gafchromic.com].
30. Shehzadi NN, Yi C-Y, Kim K-H, Jang J, Hwang U-J, Kim Y, et al. Feasibility study of radiophotoluminescent glass dosimeter for in vivo dosimetry in external photon beam radiotherapy. *J Korean Phys Soc.* 2021;78(6):523-34.
31. Siemens. Computed Tomography, Somatom Definitions [Available from: <https://www.siemens-healthineers.com/en-us/computed>].
32. Akbas U, Kesen N, Koksal C, Özkaya Toraman K, Altun M, Bilge H. Investigation of Surface Dose Using Film Dosimetry and Commercial Treatment Planning System for Larynx Cancer Treatment with Intensity-Modulated Radiotherapy and Volumetric Modulated Arc Therapy. *Turkish Journal of Oncology.* 2018;33.
33. Oonsiri P, Kingkaew S, Vannavijit C, Suriyapee S. Investigation of the dosimetric characteristics of radiophotoluminescent glass dosimeter for high-energy photon beams. *Journal of Radiation Research and Applied Sciences.* 2019;12(1):65-71.
34. Son K, Jung H, Shin SH, Lee H-H, Kim M-S, Ji YH, et al. Evaluation of the dosimetric characteristics of a radiophotoluminescent glass dosimeter for high-energy

photon and electron beams in the field of radiotherapy. Radiation Measurements. 2011;46(10):1117-22.

35. Qi ZY, Deng XW, Huang SM, Zhang L, He ZC, Li XA, et al. In vivo verification of superficial dose for head and neck treatments using intensity-modulated techniques. Med Phys. 2009;36(1):59-70.

36. Bilge H, Cakir A, Okutan M, Acar H. Surface dose measurements with GafChromic EBT film for 6 and 18MV photon beams. Phys Med. 2009;25(2):101-4.

37. Commissioning and Quality Assurance of Computerized Planning Systems for Radiation Treatment of Cancer. Vienna: INTERNATIONAL ATOMIC ENERGY AGENCY; 2004.



VITA

NAME	Sonam Choki
DATE OF BIRTH	6 February 1990
PLACE OF BIRTH	Thimphu, Bhutan
INSTITUTIONS ATTENDED	<ul style="list-style-type: none"> - Bachelors in Radiology and Imaging Science Technology Naresuan University, Phitsanulok, Thailand - Master of Science in Medical Physics, Faculty of Medicine, Department of Radiology, Chulalongkorn University, Bangkok, Thailand - National Cancer Institute, Thailand - Department of Radiation Oncology, JDWNRH, Bhutan
HOME ADDRESS	Faculty of Medicine, 1873 Rama 4 Road, Pathumwan District, Bangkok, 10330 Chulalongkorn University, Bangkok, Thailand
PUBLICATION	Choki S, Sanghangthum T. Surface and Buildup Doses Comparison between Analytical Anisotropic Algorithm and Acuros XB for Various Treatment Parameters in Proceedings of 20th Asia-Oceania Congress on Medical Physics 2020(AOCMP) - 18th South-East Asia Congress of Medical Physics(SEACOMP) - 12th Annual Meeting of Thai Medical Physicist Society(TMPS), Phuket, Thailand, 2020